

Electronic Supplementary Information (ESI)

Boron-based donor-spiro-acceptor compounds exhibiting thermally activated delayed fluorescence (TADF)

Marco Stanoppi, Andreas Lorbach*

E-Mail: andreas.lorbach@uni-konstanz.de

Universität Konstanz, Fachbereich Chemie,
Universitätsstr. 10, 78464 Konstanz, Germany

Table of content

S1	Syntheses	S3
S1.1	Materials and general methods.....	S3
S1.2	Syntheses of precursors	S4
S1.3	Syntheses of emitters 1 , 2 , 2^F , and 3	S6
S2	Single-crystal X-ray crystallography	S9
S3	DFT calculations	S11
S4	Photoluminescence measurements	S14
S4.1	Time-correlated single-photon counting (TCSPC) experiments.....	S15
S5	NMR spectra	S18
S6	References.....	S27

S1 Syntheses

S1.1 Materials and general methods

Unless otherwise specified the syntheses were conducted under inert atmosphere by means of standard Schlenk techniques or in an *MBraun Labstar* glovebox operating under nitrogen atmosphere with monitored amounts of water and oxygen. Commercially available chemicals were used as received unless otherwise indicated. Solvents were distilled from the appropriate drying agents: THF (sodium-benzophenone), toluene (sodium-benzophenone), *n*-hexane (sodium), and DCM (calcium hydride). All the indicated solvents were stored under inert conditions over 4 Å molecular sieves and their water contents were attested to be below 10 ppm by means of coulometric Karl Fischer titrations (*SI Analytics TitroLine 7500 KF trace*).

n-BuLi was titrated prior use with menthol (isomeric mixture) and 2,2'-bipyridine as indicator, Me₂SnCl₂ was sublimed under reduced pressure and stored under nitrogen atmosphere.

Anhydrous MgBr₂ in THF (0.2 M) was freshly prepared prior use: to a suspension of Mg turnings in the appropriate amount of THF, a stoichiometric amount of 1,2-dibromoethane was slowly added dropwise, keeping the temperature constant at r.t. by means of a water bath. The reaction was considered complete after gas evolution ceased.

2-(2-Dibromoborylphenyl)pyridine (**4**),¹ (2,4-difluorophenyl)pyridine borane dibromide complex (**dfppyBBr₂**),² 2,2'-dilithio-diphenyl sulfide · 2 TMEDA³ and *N,N*-bis(2-lithiophenyl)methylamine · TMEDA³ were synthesized according to previously reported procedures.

Flash column chromatography was performed using the automated system *Interchim puriFlash XS 420+* with self-packed silica gel columns. The *R_f* values are referring to TLC plates with the same stationary phase.

NMR spectra were recorded in deuterated solvents on *Bruker Avance III-400* or *Bruker Avance III HD-400* spectrometers. Chemical shifts are reported as dimensionless δ values in ppm and ¹H NMR spectra are referenced relative to residual *protio*-solvent signals (CD₂Cl₂: 5.32 ppm; CDCl₃: 7.26 ppm). The remaining nuclei are referenced using the unified scale as defined by IUPAC⁴ with the following values for Ξ : ¹¹B (Ξ = 32.083974; BF₃·OEt₂), ¹³C (Ξ = 25.145020; Me₄Si), ¹⁹F (Ξ = 94.094011; CCl₃F), ¹¹⁹Sn (Ξ = 37.290632; Me₄Sn).

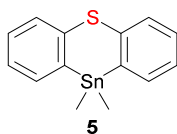
Carbon atoms directly bonded to boron are not always observed in the ¹³C{¹H} NMR spectra due to quadrupolar relaxation leading to considerable signal broadening. Abbreviations: s = singlet, d = doublet, t = triplet, m = multiplet, n. o. = not observed.

HRMS (ESI⁺) were obtained using a *Thermo Scientific Velos Pro* mass spectrometer.

Elemental analyses were performed on an *Elementar vario EL cube*.

S1.2 Syntheses of precursors

Synthesis of 10,10-dimethylphenothiastannin (5)



The synthesis was performed following a modified version of the procedure reported by Meinema and Noltes.⁵

2,2'-Dilithio-diphenyl sulfide · 2 TMEDA (1.20 g, 2.8 mmol) was suspended in 100 mL toluene. Me₂SnCl₂ (0.61 g, 2.8 mmol) was dissolved in 40 mL toluene and added dropwise to the suspension at r.t. The turbid mixture turned from orange to colorless at the end of the addition. The suspension was then heated to reflux for 2 h and stirred at r.t. overnight. The reaction mixture was poured on ice and the aqueous phase was extracted with toluene (3 × 50 mL). The combined organic phases were dried over MgSO₄, filtered, and the solvent was evaporated.

Purification of the crude product *via* flash column chromatography using *n*-hexane as eluent (*R_f* = 0.35, *n*-hexane) gave the desired product as a colorless solid (0.546 g, 1.64 mmol, 59% yield).

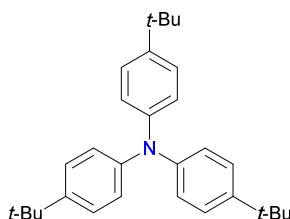
¹H NMR (400 MHz, CD₂Cl₂): δ 7.70–7.63 (2H, m), 7.61–7.53 (2H, m), 7.30–7.22 (4H, m), 0.57 (6H, s, *J*_{H¹¹⁷Sn} = 60.2 Hz, *J*_{H¹¹⁷Sn} = 57.6 Hz).

¹³C{¹H} NMR (101 MHz, CD₂Cl₂): δ 145.35, 143.26, 136.00, 130.42, 128.82, 126.98, –10.70.

¹¹⁹Sn NMR (149 MHz, CD₂Cl₂): δ –105.32.

Anal. calc. for C₁₄H₁₄SSn (333.04 g/mol): C, 50.49; H, 4.24. Found: C, 50.48; H, 4.24.

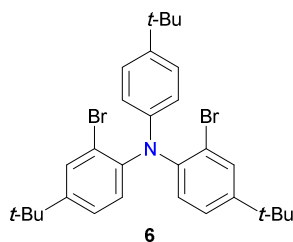
Synthesis of tris(4-*tert*-butylphenyl)amine



The synthesis was performed following a modified version of the procedure reported by Rathore *et al.*⁶

A mixture of triphenylamine (14.7 g, 60 mmol), *tert*-butanol (46.7 g, 630 mmol), and trifluoroacetic acid (180 mL) was stirred at 50 °C overnight. During this time a green precipitate formed. A saturated aqueous NaHCO₃ solution was pre-cooled in an ice-water bath and the reaction mixture was slowly added into this solution. The aqueous phase was extracted with toluene (3 × 100 mL) and the combined organic phases were dried over MgSO₄, filtered, and the solvent was removed under reduced pressure. The so obtained yellow solid was washed three times with *n*-hexane. The desired compound was isolated as an off-white powder (21.0 g, 50.8 mmol, 85% yield). NMR spectroscopic data well match those previously reported.⁶

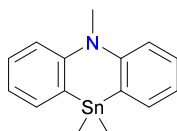
Synthesis of 6



The synthesis was performed following a modified version of the procedure reported by Clark *et al.*⁷

Tris-(4-*tert*-butylphenyl)amine (5.0 g, 12 mmol) was dissolved in DCM (210 mL). *N*-bromosuccinimide (4.5 g, 25.3 mmol) in DMF (48 mL) was added slowly and the solution was stirred at r.t. overnight. The solution was washed with water (5 × 100 mL) and the combined organic phases were dried over MgSO₄, filtered, and the solvent was evaporated. The product was obtained as an off-white powder (5.65 g, 9.89 mmol, 82% yield). NMR spectroscopic data well match those previously reported.⁷

Synthesis of 5,10,10-trimethyl-5,10-dihydrophenazastannin



The synthesis was performed following a modified version of the procedure reported by Kupchik and Perciaccante.⁸

N,N-bis(2-lithiophenyl)methylamine · TMEDA (1.90 g, 6.10 mmol) was suspended in 60 mL toluene. Me₂SnCl₂ (1.31 g, 5.96 mmol) was dissolved in 40 mL toluene and added dropwise to the aforementioned suspension at r.t. The mixture turned from orange to colorless at the end of the addition. The suspension was then heated to reflux for 3 h and stirred at r.t. overnight. The reaction mixture was poured on ice and the aqueous phase was extracted with toluene (3 × 50 mL). The combined organic phases were dried over MgSO₄, filtered, and the solvent was evaporated. The product was obtained as a colorless powder (1.30 g, 3.94 mmol, 66% yield). No further purification steps were needed and ¹H NMR spectroscopic data are in agreement with those previously reported (¹³C and ¹¹⁹Sn NMR data were not given).⁸

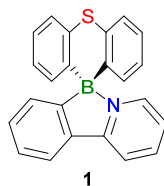
¹H NMR (400 MHz, CDCl₃): δ 7.47 (2H, dd, *J* = 7.1 Hz, *J* = 1.7 Hz), 7.32 (2H, ddd, *J* = 8.2 Hz, *J* = 7.2 Hz, *J* = 1.8 Hz), 7.19 (2H, d, *J* = 8.2 Hz), 7.03 (2H, td, *J* = 7.1 Hz, *J* = 1.0 Hz), 3.47 (3H, s), 0.50 (6H, s, *J*_{H¹¹⁹Sn} = 60.3, *J*_{H¹¹⁷Sn} = 57.6).

¹³C{¹H} NMR (101 MHz, CDCl₃): δ 153.80, 135.73, 132.10, 129.17, 121.98, 117.16, 40.07, -10.48.

¹¹⁹Sn NMR (149 MHz, CDCl₃): δ -117.87.

S1.3 Syntheses of emitters 1, 2, 2^F, and 3

Synthesis of 1



5 (0.443 g, 1.33 mmol) and **4** (0.432 g, 1.33 mmol) were dissolved in 30 mL DCM and, under stirring, AlCl₃ (0.017 g, 0.13 mmol) was added. The mixture was stirred overnight at r.t. and the solvent was evaporated. The crude product was recrystallized three times by adding *n*-hexane to DCM solutions to give a colorless solid (0.334 g, 0.96 mmol, 72% yield). (*R*_f = 0.17, DCM/hexane, 1:3).

HRMS (ESI, *m/z*) calc. for [C₂₃H₁₆BNS]⁺: 349.1091, found: 349.1090.

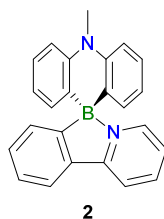
Anal. calc. for C₂₃H₁₆BNS (349.26 g/mol): C, 79.10; H, 4.62; N, 4.01. Found: C, 78.91; H, 4.59; N, 4.17.

¹H NMR (400 MHz, CDCl₃): δ 8.63 (1H, d, *J* = 5.8 Hz), 8.00–7.95 (2H, m), 7.93 (1H, d, *J* = 7.5 Hz), 7.71 (1H, d, *J* = 7.2 Hz), 7.48 (2H, d, *J* = 7.5 Hz), 7.46 (1H, m), 7.42 (1H, td, *J* = 7.4 Hz, *J* = 0.9 Hz), 7.21 (1H, td, *J* = 6.1 Hz, *J* = 2.4 Hz), 7.13 (2H, td, *J* = 7.5 Hz, *J* = 1.3 Hz), 6.90 (2H, t, *J* = 7.4 Hz), 6.69 (2H, d, *J* = 7.4 Hz).

¹³C{¹H} NMR (101 MHz, CDCl₃): δ 157.43, 144.65, 140.61, 138.17, 136.99, 132.90, 131.55, 131.41, 126.58, 126.51, 125.59, 124.95, 122.54, 121.56, 117.78, n. o. (BC).

¹¹B NMR (128 MHz, CDCl₃): δ 0.60.

Synthesis of 2



The synthesis was performed following the same procedure employed for compound **1**, reacting 5,10,10-trimethyl-5,10-dihydrophenazastannin (0.200 g, 0.61 mmol), **4** (0.197 g, 0.61 mmol), and AlCl₃ (0.008 g, 0.06 mmol) in 15 mL DCM. The crude mixture was purified *via* flash column chromatography, using *n*-hexane and DCM as eluent that gave the pure product as a yellow solid (0.107 g, 0.31 mmol, 51% yield). (*R*_f = 0.4, DCM/hexane, 1:1).

HRMS (ESI, *m/z*) calc. for [C₂₄H₁₉BN₂+H]⁺: 347.1714, found: 347.1704.

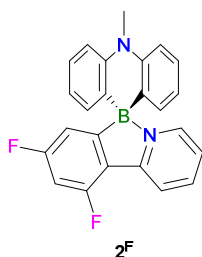
Anal. calc. for C₂₄H₁₉BN₂ (346.24 g/mol): C, 83.26; H, 5.53; N, 8.09. Found: C, 83.02; H, 5.58; N, 8.10.

¹H NMR (400 MHz, CD₂Cl₂): δ 8.15 (1H, dt, *J* = 5.7 Hz, *J* = 1.0 Hz), 8.03–7.91 (3H, m), 7.53 (1H, d, *J* = 7.1 Hz), 7.47 (1H, td, *J* = 7.1 Hz, *J* = 1.2 Hz), 7.43 (1H, td, *J* = 7.3 Hz, *J* = 1.5 Hz), 7.24–7.15 (3H, m), 7.11 (2H, d, *J* = 8.2 Hz), 6.69–6.60 (4H, m), 3.64 (3H, s).

¹³C{¹H} NMR (101 MHz, CD₂Cl₂): δ 156.69, 147.55, 143.99, 140.41, 137.26, 132.09, 131.16, 130.92, 127.10, 126.21, 122.56, 121.56, 119.20, 117.79, 112.60, 34.88, n. o. (BC).

¹¹B NMR (128 MHz, CD₂Cl₂): δ 0.02.

Synthesis of 2^F



The synthesis was performed following the same procedure employed for compound **1**, reacting 5,10,10-trimethyl-5,10-dihydrophenazastannin (0.100 g, 0.30 mmol), **dfppyBBr₂** (0.110 g, 0.30 mmol), and AlCl₃ (0.004 g, 0.03 mmol) in 10 mL DCM. The crude mixture was purified *via* flash column chromatography (*n*-hexane/DCM gradient), which gave the analytically pure product as a yellow solid (0.034 g, 0.090 mmol, 30% yield). (*R_f* = 0.19, DCM/hexane, 1:3).

HRMS (ESI, *m/z*) calc. for [C₂₄H₁₇BF₂N₂+H]⁺: 383.1526, found: 383.1515.

Anal. calc. for C₂₄H₁₇BF₂N₂ (382.22 g/mol): C, 75.42; H, 4.48; N, 7.33. Found: C, 75.39; H, 4.36; N, 7.56.

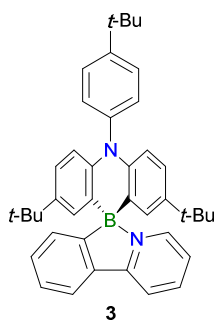
¹H NMR (400 MHz, CD₂Cl₂): δ 8.19–8.13 (2H, m), 8.00 (1H, td, *J* = 7.8 Hz, *J* = 1.5 Hz), 7.25–7.19 (3H, m), 7.12 (2H, d, *J* = 8.2 Hz), 7.01 (1H, dd, *J* = 7.7 Hz, *J* = 2.2 Hz), 6.86 (1H, ddd, *J* = 10.8 Hz, *J* = 9.2 Hz, *J* = 2.2 Hz), 6.69 (2H, td, *J* = 7.1 Hz, *J* = 1.0 Hz), 6.64 (2H, dd, *J* = 7.3 Hz, *J* = 1.9 Hz), 3.64 (3H, s).

¹³C{¹H} NMR (101 MHz, CD₂Cl₂): δ 165.26 (dd, *J_{CF}* = 255.7 Hz, *J_{CF}* = 8.7 Hz), 160.01 (dd, *J_{CF}* = 259.4 Hz, *J_{CF}* = 11.9 Hz), 152.73 (d, *J_{CF}* = 5.3 Hz), 147.29, 144.17, 141.02, 131.95, 127.41, 122.60, 121.39 (d, *J_{CF}* = 9.8 Hz), 120.40 (dd, *J_{CF}* = 7.6 Hz, *J_{CF}* = 2.3 Hz), 119.34, 113.12 (dd, *J_{CF}* = 19.3 Hz, *J_{CF}* = 3.3 Hz), 112.79, 101.73 (dd, *J_{CF}* = 27.6 Hz, *J_{CF}* = 23.8 Hz), 34.90, n. o. (BC).

¹⁹F NMR (376 MHz, CD₂Cl₂): δ -106.19 (d, *J_{FF}* = 9.5 Hz), -114.10 (d, *J_{FF}* = 9.5 Hz).

¹¹B NMR (128 MHz, CD₂Cl₂): δ 0.14.

Synthesis of 3



A solution of **6** (0.50 g, 0.88 mmol) in THF (30 mL) was cooled to -78 °C using an isopropanol-dry ice bath and *n*-BuLi (2.4 M in *n*-hexane, 0.73 mL, 1.8 mmol) was then added dropwise. The mixture was stirred at the same temperature for 1 h. After this time, MgBr₂ (0.20 M in THF, 7.3 mL, 1.5 mmol) was added dropwise, at the end of the addition the flask was removed from the cooling bath and stirred for 30 min at r.t. The reaction mixture was then slowly added to a solution of **4** (0.237 g, 0.73 mmol) in THF (20 mL) *via* a PTFE cannula. After the addition, the mixture was stirred for 2 d at r.t. The reaction was then quenched with distilled water and the aqueous phase was extracted with toluene (3 × 50 mL). The combined organic phases were dried over MgSO₄, filtered, and the solvent was evaporated. The crude product was purified *via* flash column chromatography (*n*-hexane/DCM gradient) to give an orange solid (0.137 g, 0.238 mmol, 33% yield). (*R_f* = 0.16, DCM/hexane, 1:3).

HRMS (ESI, *m/z*) calc. for [C₄₁H₄₅BN₂+H]⁺: 577.3749, found: 577.3732.

Anal. calc. for C₄₁H₄₅BN₂ (576.64 g/mol): C, 85.40; H, 7.87; N, 4.86. Found: C, 85.37; H, 7.40; N, 4.90.

^1H NMR (400 MHz, CDCl_3): δ 8.27 (1H, d, $J = 5.7$ Hz), 7.98 (2H, d, $J = 7.8$ Hz), 7.90 (1H, td, $J = 7.7$ Hz, $J = 1.3$ Hz), 7.70 (1H, d, $J = 7.2$ Hz), 7.64 (2H, d, $J = 8.4$ Hz), 7.49 (1H, td, $J = 7.1$ Hz, $J = 1.0$ Hz), 7.43 (1H, td, $J = 7.4$ Hz, $J = 1.1$ Hz), 7.36 (2H, d, $J = 8.4$ Hz), 7.14 (1H, ddd, $J = 7.3$ Hz, $J = 5.6$ Hz, $J = 1.0$ Hz), 6.99 (2H, dd, $J = 8.7$ Hz, $J = 2.5$ Hz), 6.69 (2H, d, $J = 2.5$ Hz), 6.32 (2H, d, $J = 8.7$ Hz), 1.46 (9H, s), 1.03 (18H, s).

$^{13}\text{C}\{^1\text{H}\}$ NMR (101 MHz, CDCl_3): δ 156.42, 150.30, 145.26, 144.87, 140.92, 140.66, 139.72, 137.16, 131.92, 131.03, 130.88, 129.95, 127.44, 125.95, 123.55, 122.28, 121.03, 117.23, 113.66, 34.76, 33.68, 31.56, 31.41, n. o. (BC).

^{11}B NMR (128 MHz, CDCl_3): δ 0.58.

S2 Single-crystal X-ray crystallography

1, **2**, **2^F**, and **3** were crystallized by layering DCM solutions with *n*-hexane. Suitable crystals were selected and mounted on *MiTeGen Dual-Thickness MicroMounts* in paraffin oil on a *STOE IPDS 2T* diffractometer equipped with a graphite-monochromated radiation source and an image plate detector. The crystals were kept at 100 K during data collection. The structures were solved with the *ShelXS* structure solution program⁹ using Direct Methods and refined with the *ShelXL* refinement package¹⁰ using Least Squares minimization within the software *Olex2*¹¹.

Table S1 Crystallographic data for **1–3**.

	1	2	2^F	3 · 0.5 CH₂Cl₂
CCDC	1830512	1830513	1830514	1830515
Chemical formula	C ₂₃ H ₁₆ BNS	C ₂₄ H ₁₉ BN ₂	C ₂₄ H ₁₇ BF ₂ N ₂	C ₄₁ H ₄₅ BN ₂ · 0.5 CH ₂ Cl ₂
<i>M_r</i> [g mol ⁻¹]	349.24	346.22	382.20	619.06
<i>T</i> [K]	100(1)	100(1)	100(1)	100(1)
Crystal system	monoclinic	monoclinic	triclinic	triclinic
Space group	<i>P</i> 2 ₁	<i>C</i> c	<i>P</i> $\bar{1}$	<i>P</i> $\bar{1}$
<i>a</i> [Å]	8.6076(3)	10.4501(8)	9.0580(6)	7.7660(4)
<i>b</i> [Å]	9.4500(5)	24.7509(16)	10.2042(7)	13.7779(7)
<i>c</i> [Å]	10.8046(4)	8.0062(6)	10.5865(7)	17.7144(9)
α [°]	90	90	72.129(5)	70.971(4)
β [°]	99.428(3)	120.520(5)	79.861(5)	82.959(4)
γ [°]	90	90	78.732(5)	89.145(4)
<i>V</i> [Å ³]	866.99(6)	1783.9(2)	906.25(11)	1777.70(16)
<i>Z</i>	2	4	2	2
ρ_{calcd} [g cm ⁻³]	1.338	1.289	1.401	1.157
μ [mm ⁻¹]	0.192	0.075	0.096	0.138
<i>F</i> (000)	364.0	728.0	396.0	662.0
Crystal size [mm ³]	0.30 × 0.275 × 0.275	0.45 × 0.375 × 0.15	0.50 × 0.35 × 0.20	0.45 × 0.35 × 0.30
Radiation type	Mo <i>K</i> α (λ = 0.71073 Å)			
2 θ range for data collection [°]	4.798–60.538	5.562–57.112	4.622–58.108	4.562–54.182
Index ranges	–12 ≤ <i>h</i> ≤ 12,	–13 ≤ <i>h</i> ≤ 14,	–12 ≤ <i>h</i> ≤ 12,	–9 ≤ <i>h</i> ≤ 9, –17 ≤
	–13 ≤ <i>k</i> ≤ 13,	–33 ≤ <i>k</i> ≤ 33,	–13 ≤ <i>k</i> ≤ 13,	<i>k</i> ≤ 17, –22 ≤ <i>l</i> ≤
	–15 ≤ <i>l</i> ≤ 15	–10 ≤ <i>l</i> ≤ 10	–14 ≤ <i>l</i> ≤ 14	22
Reflections collected	14213	12068	13692	27942
No. of independent reflections (<i>R</i> _{int} , <i>R</i> _{sigma})	5160 (0.0259, 0.0244)	4527 (0.0510, 0.0496)	4820 (0.0304, 0.0280)	7774 (0.0360, 0.0389)
Data/restraints/parameters	5160/1/235	4527/2/245	4820/51/307	7774/262/530
Goodness-of-fit on <i>F</i> ²	1.044	1.009	1.099	1.023
<i>R</i> ₁ , <i>wR</i> ₂ (<i>I</i> ≥ 2 σ (<i>I</i>))	0.0275, 0.0695	0.0450, 0.0912	0.0460, 0.1228	0.0497, 0.1152
<i>R</i> ₁ , <i>wR</i> ₂ (all data)	0.0303, 0.0705	0.0616, 0.0966	0.0569, 0.1264	0.0766, 0.1241
Largest diff. peak/hole [e Å ⁻³]	0.25/–0.21	0.17/–0.19	0.27/–0.22	0.41/–0.30
Flack parameter	–0.01(2)	–0.7(10)		

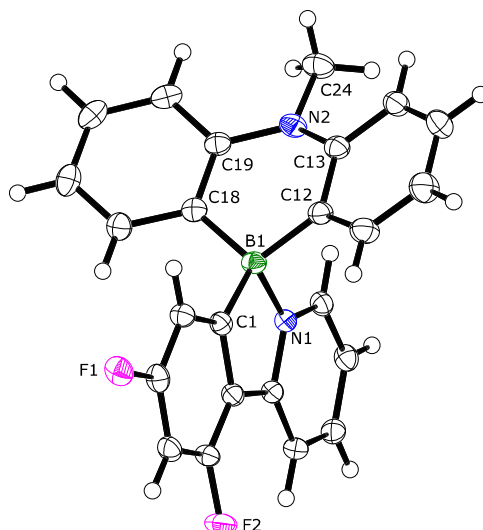


Figure S1 Solid-state structure of **2F**. Displacement ellipsoids are drawn at the 50% probability level. The fluorinated 2-phenylpyridine is disordered over two positions and only the major component (93%) is shown. The minor component was refined isotropically and its relative geometry was restrained to the geometry of the major component by using the *SAME* command. Selected bond lengths [Å] and dihedral angle [°]: B1–N1: 1.638(2), B1–C1: 1.610(3), B1–C12: 1.601(2), B1–C18: 1.603(2); Ph(C12)//Ph(C18) = 31.52(7).

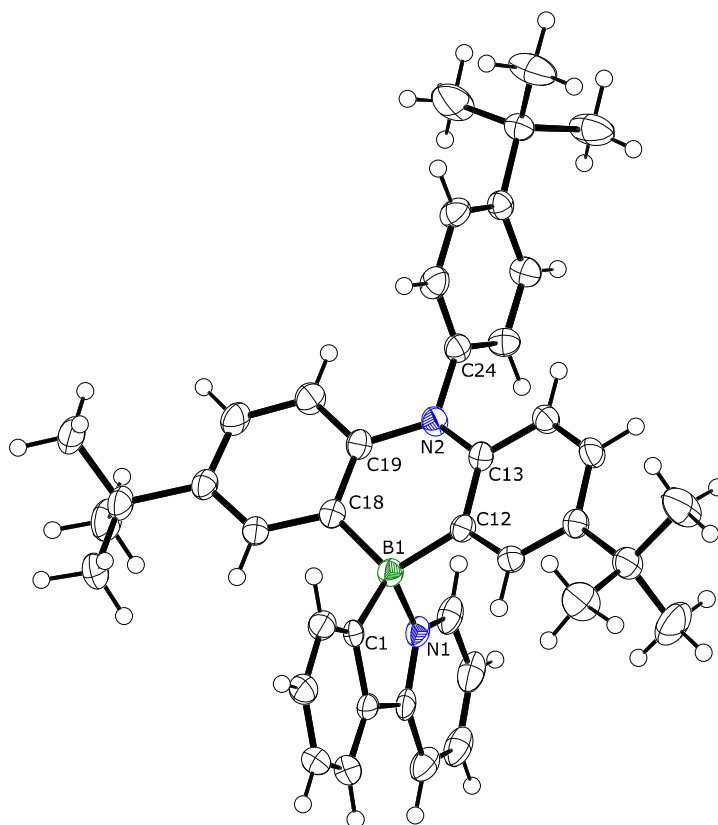
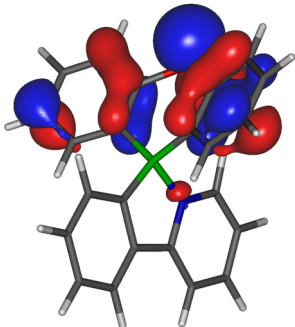
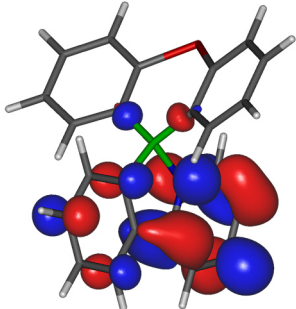
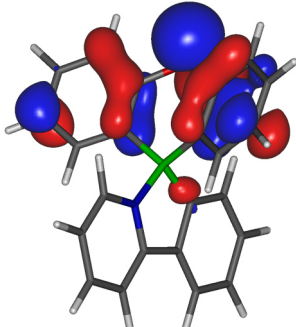
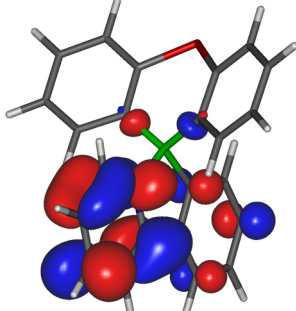
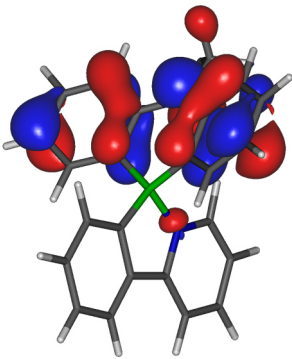
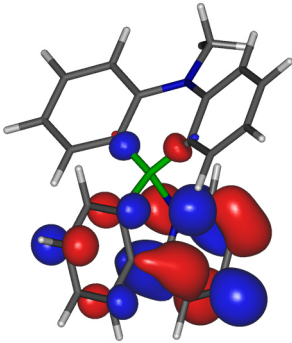
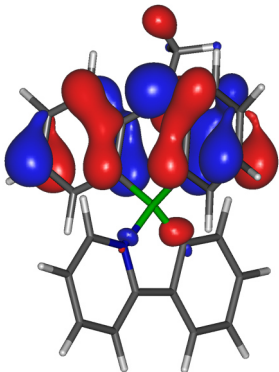
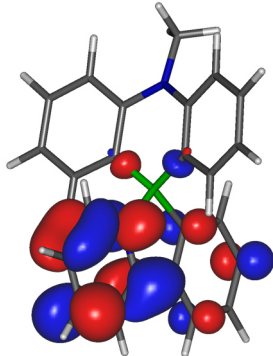
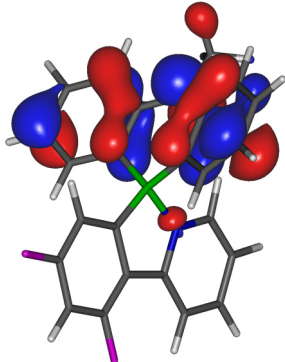
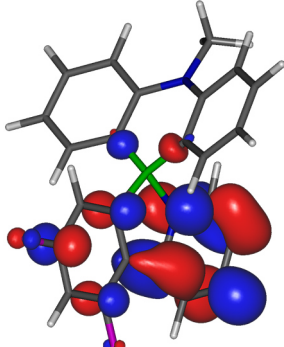


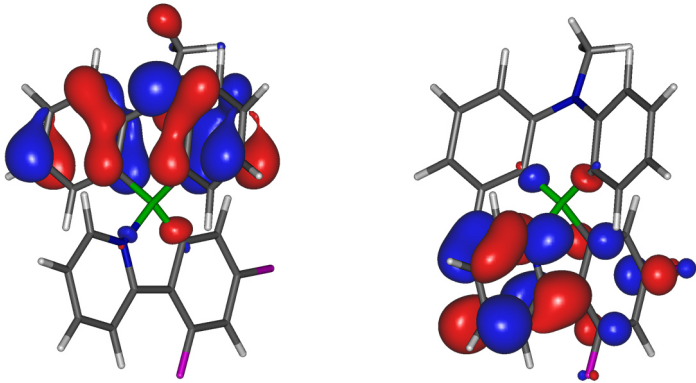
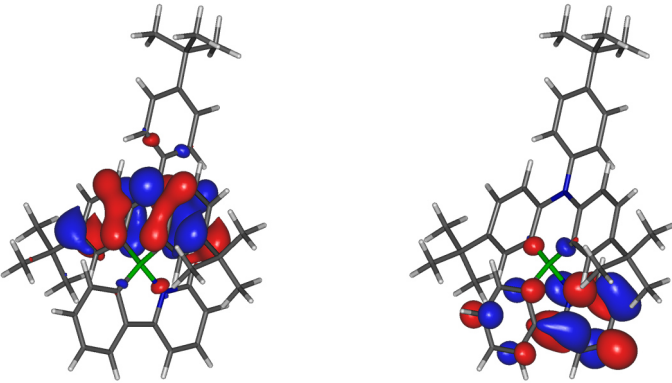
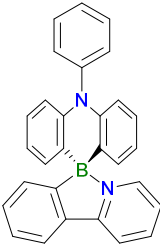
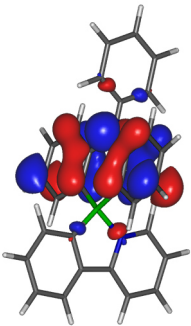
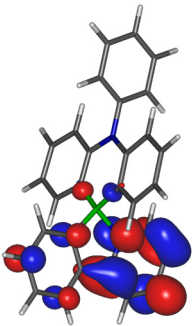
Figure S2 Solid-state structure of **3 · 0.5 CH₂Cl₂**. The CH₂Cl₂ molecule is located on the crystallographic inversion center and omitted for clarity. Displacement ellipsoids are drawn at the 50% probability level. The 2-phenylpyridine is disordered over two positions and only the major component (65%) is shown. The relative geometry of the disordered fragment was restrained to the geometry of the major component by using the *SAME* command. Selected bond lengths [Å] and dihedral angle [°]: B1–N1: 1.596(11), B1–C1: 1.626(15), B1–C12: 1.599(2), B1–C18: 1.600(2); Ph(C12)//Ph(C18) = 18.83(9).

S3 DFT calculations

Table S2 Orbital representations (isovalue = 0.04),¹² orbital energies, and selected structural parameters for **1–3** (cf. Fig. 2 for the definition of ϕ). Calculations were performed at the B3LYP/6-31+G* level of theory using the Gaussian 16 program (Revision B.01).¹³ Initial molecular geometries were derived from single-crystal X-ray crystallography and then optimized at the B3LYP/6-31G* level of theory. In order to reduce the computational expense, the optimized structures were symmetrized¹² (C_s point group; rotation of one *tert*-Bu group was necessary in the case of **3**) before optimization at the B3LYP/6-31+G* level of theory. Harmonic frequency calculations on the resulting geometries confirmed that these are local minima on the potential energy surface.

	HOMO	LUMO
1 (Isomer 1) Energy (eV) B–N (Å) ϕ (°) Donor Ph//Ph (°)	 –5.38 1.664 88.5 27.2	 –2.18
1 (Isomer 2) Energy (eV) B–N (Å) ϕ (°) Donor Ph//Ph (°)	 –5.24 1.626 24.7 30.6	 –2.30

	HOMO	LUMO
2 (Isomer 1) Energy (eV) B-N (Å) ϕ (°) Donor Ph//Ph (°)	 -4.96 1.669 87.2 26.8	 -2.07
2 (Isomer 2) Energy (eV) B-N (Å) ϕ (°) Donor Ph//Ph (°)	 -4.82 1.643 40.5 21.0	 -2.13
2^F (Isomer 1) Energy (eV) B-N (Å) ϕ (°) Donor Ph//Ph (°)	 -5.10 1.665 86.0 26.1	 -2.25

	HOMO	LUMO
<p>2^F (Isomer 2)</p>  <p>Energy (eV) -4.98 B-N (Å) 1.639 ϕ (°) 39.2 Donor Ph//Ph (°) 21.4</p>		
<p>3</p>  <p>Energy (eV) -4.67 B-N (Å) 1.677 ϕ (°) 69.7 Donor Ph//Ph (°) 6.3</p>		
 <p>Energy (eV) -4.85 B-N (Å) 1.675 ϕ (°) 67.8 Donor Ph//Ph (°) 4.8</p>		

S4 Photoluminescence measurements

The doped PMMA thin films were obtained from 250 μL of a DCM solution containing the emitter and PMMA (*Sigma-Aldrich*, $M_w = 120,000$ g/mol) in concentrations of 2.1 mg/mL and 40 mg/mL, respectively. The solution was introduced in a 10 mm \times 10 mm quartz cuvette and the solvent evaporated at atmospheric pressure while the cuvette was kept horizontal and slowly spun in a way that the solution could wet all sides of the cuvette. After complete evaporation of the solvent, the cuvette was additionally kept under vacuum ($1-9 \times 10^{-3}$ mbar) for 2 h at r.t. and successively capped under nitrogen atmosphere. For the solution measurements, toluene (UV-vis spectroscopic grade) was degassed by three freeze-pump-thaw cycles.

The luminescence measurements were carried out on a *PicoQuant FluoTime 300* spectrometer. A xenon lamp was utilized as the light source for steady-state photoluminescence measurements and a pulsed LED (*PicoQuant PLS 320*) with $\lambda_{\text{exc}} = 325$ nm and a pulse width of 600 ps (for lifetimes $< 20\mu\text{s}$) or a pulsed xenon flash lamp with a pulse width of 400 ns was utilized for time-resolved measurements. The second-order diffraction band was suppressed by employing a long-pass filter (*Hoya L-38*, $\lambda_{\text{cut-on}} = 380$ nm) in the emission beam path.

All PMMA film samples and the powder sample were characterized in an integrating sphere where the sample was illuminated indirectly (out-of-beam position).

Absolute fluorescence quantum yields were determined in a calibrated integrating sphere using a xenon lamp ($\lambda_{\text{exc}} = 340$ nm) as the light source.

Absorption spectra were recorded on an *HP 8453* UV-vis spectrophotometer.

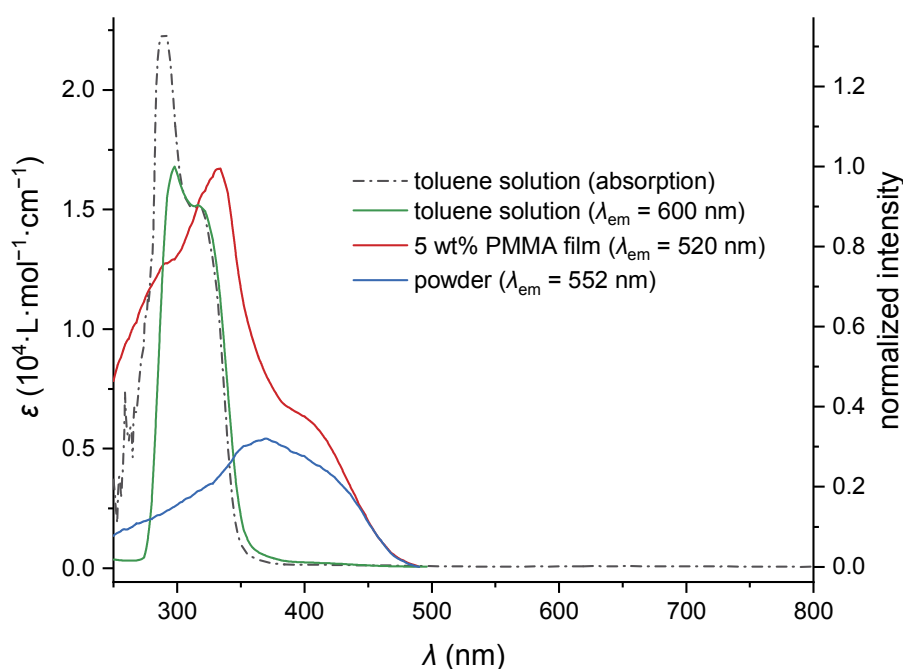


Figure S3 Absorption (broken line) and excitation spectra (solid lines) of **2**. In toluene solution, the absorption and excitation spectra superimpose well. The red-shifted excitation spectrum of **2** in a PMMA film shows a pronounced shoulder at 400 nm which is similar to the excitation spectrum of a powder sample and may indicate aggregation of **2** within the PMMA matrix.

S4.1 Time-correlated single-photon counting (TCSPC) experiments

The long-lived emissions of the toluene solutions are unequivocally identified by the curve fit of the decays even though it is hardly visible due to the low emission intensity and the resulting high background noise. In all cases, the pile-up rates were kept below 10%. The instrument response function (IRF) was utilized in the iterative reconvolution with the decay function.

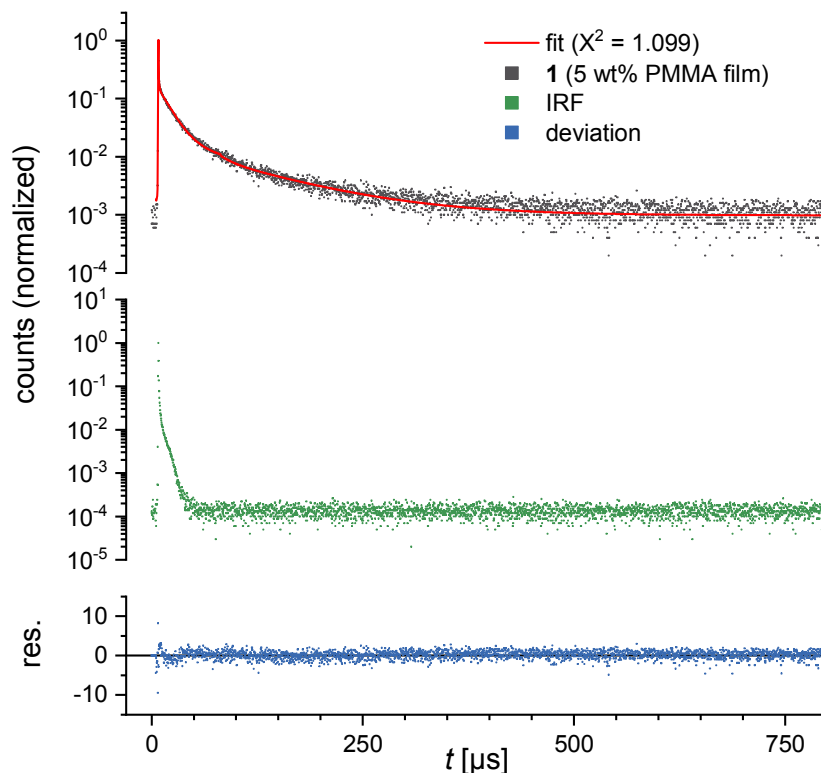


Figure S4 Excitation with a xenon flash lamp (330 nm). Optimized lifetime components: $\tau_1 = 14.0(6) \mu\text{s}$; $\tau_2 = 97(5) \mu\text{s}$.

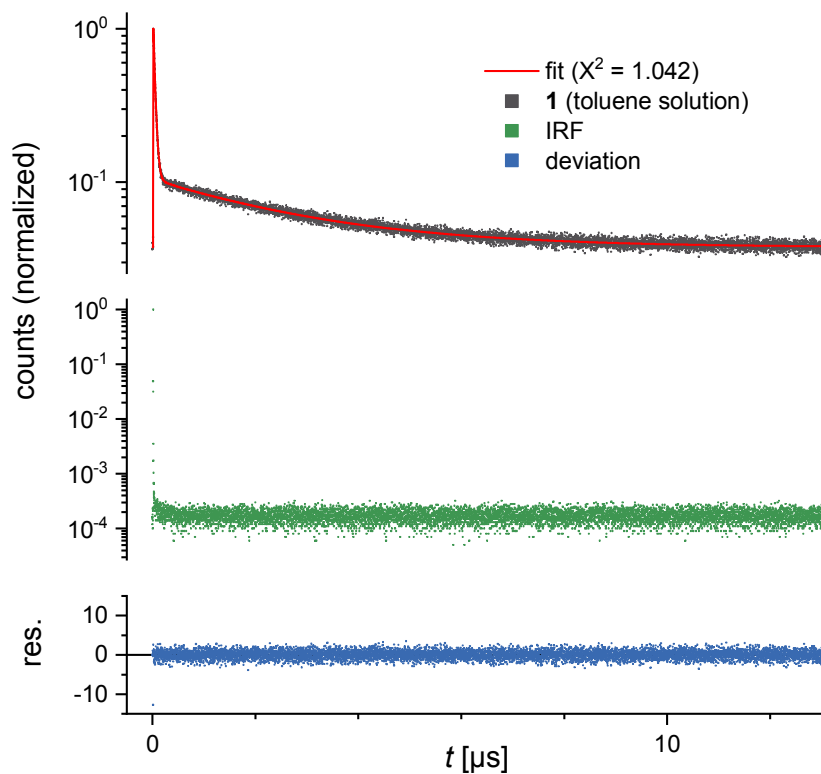


Figure S5 Excitation with a pulsed LED (325 nm). Optimized lifetime components: $\tau_1 = 34.6(12) \text{ ns}$; $\tau_2 = 2.73(7) \mu\text{s}$.

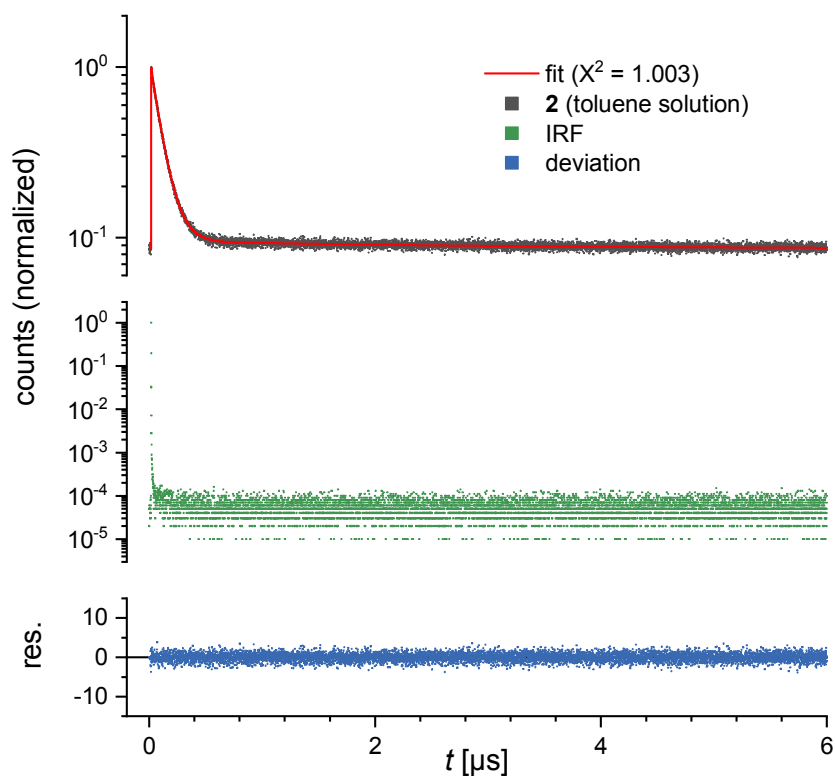


Figure S6 Excitation with a pulsed LED (325 nm). Optimized lifetime components: $\tau_1 = 91.4(15)$ ns; $\tau_2 = 2.8(5)$ μs .

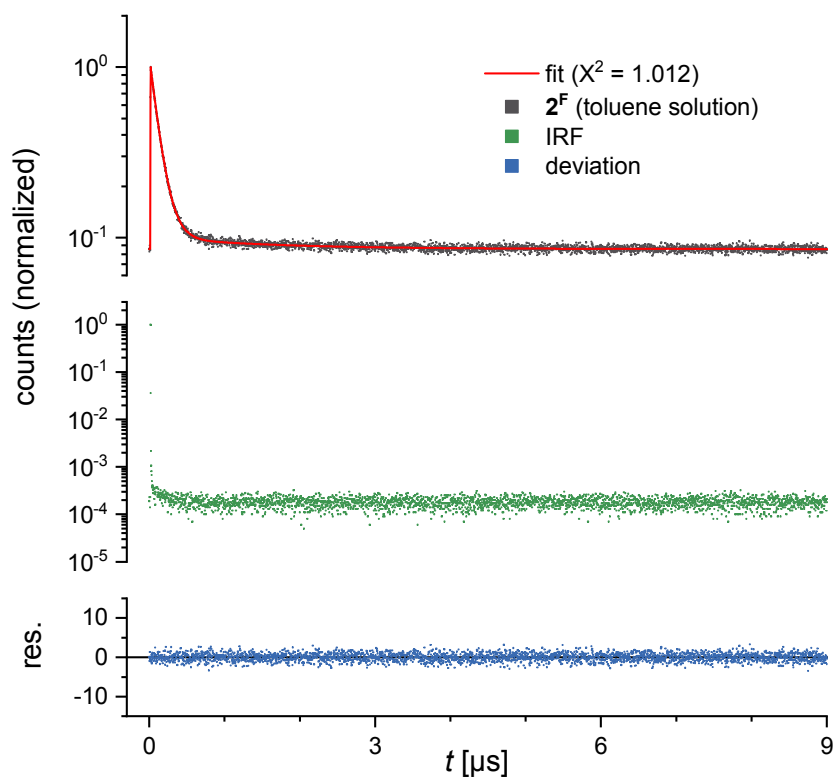


Figure S7 Excitation with a pulsed LED (325 nm). Optimized lifetime components: $\tau_1 = 110(2)$ ns; $\tau_2 = 1.5(2)$ μs .

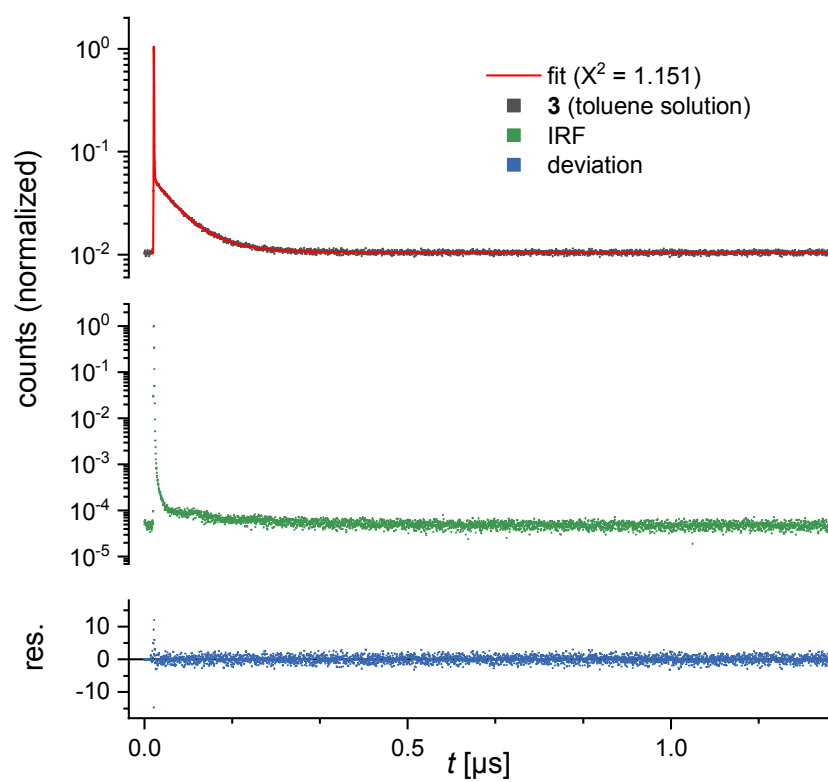


Figure S8 Excitation with a pulsed LED (325 nm). Optimized lifetime components: $\tau = 52.8(9)$ ns.

S5 NMR spectra

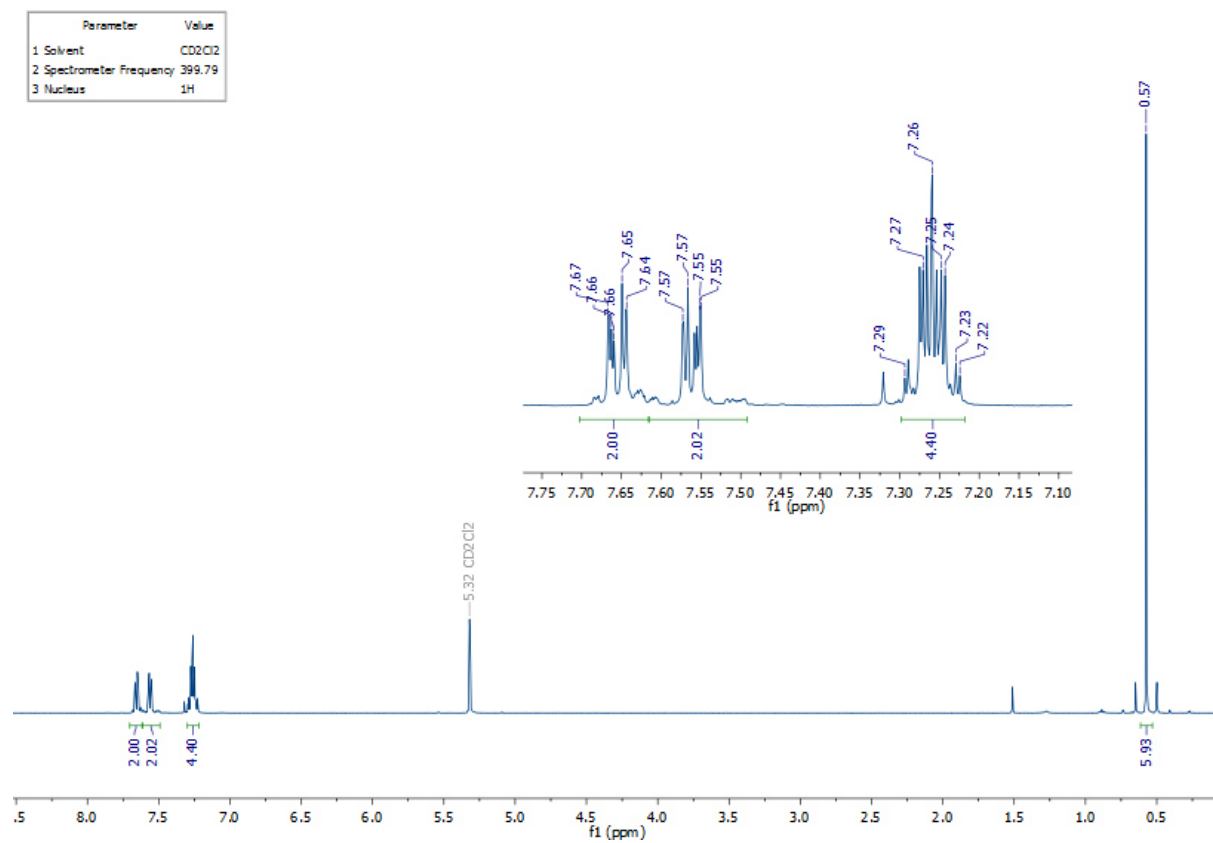


Figure S9 ¹H NMR spectrum of 10,10-dimethylphenothiastannin (5).

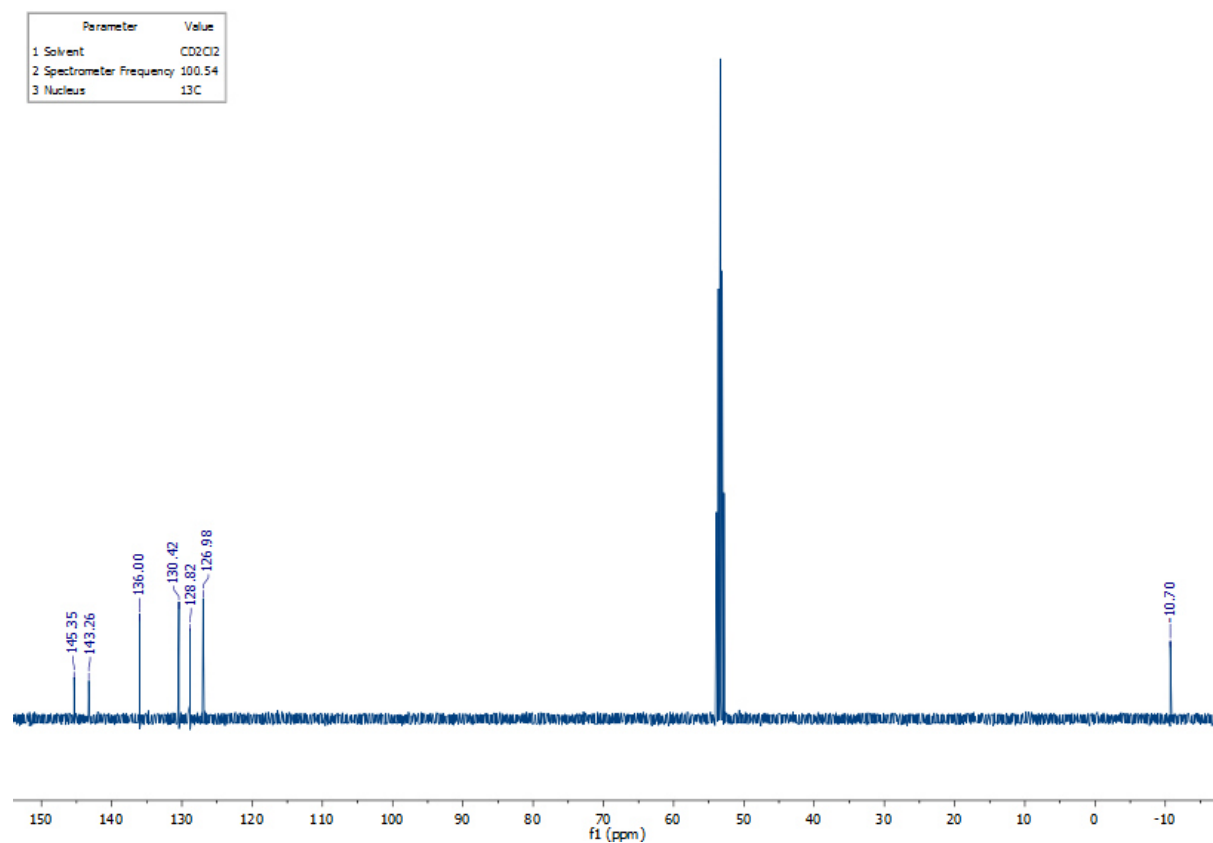


Figure S10 ¹³C{¹H} NMR spectrum of 10,10-dimethylphenothiastannin (5).

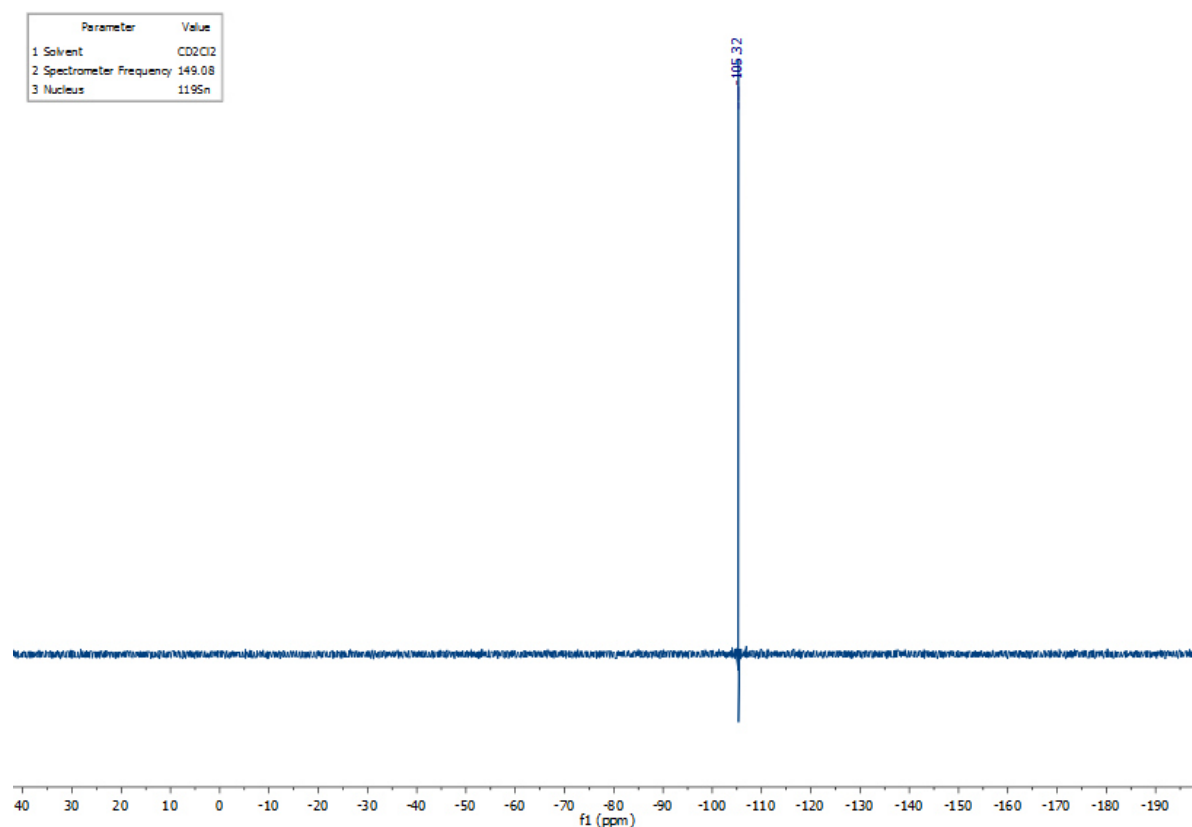


Figure S11 ¹¹⁹Sn NMR spectrum of 10,10-dimethylphenothiastannin (5).

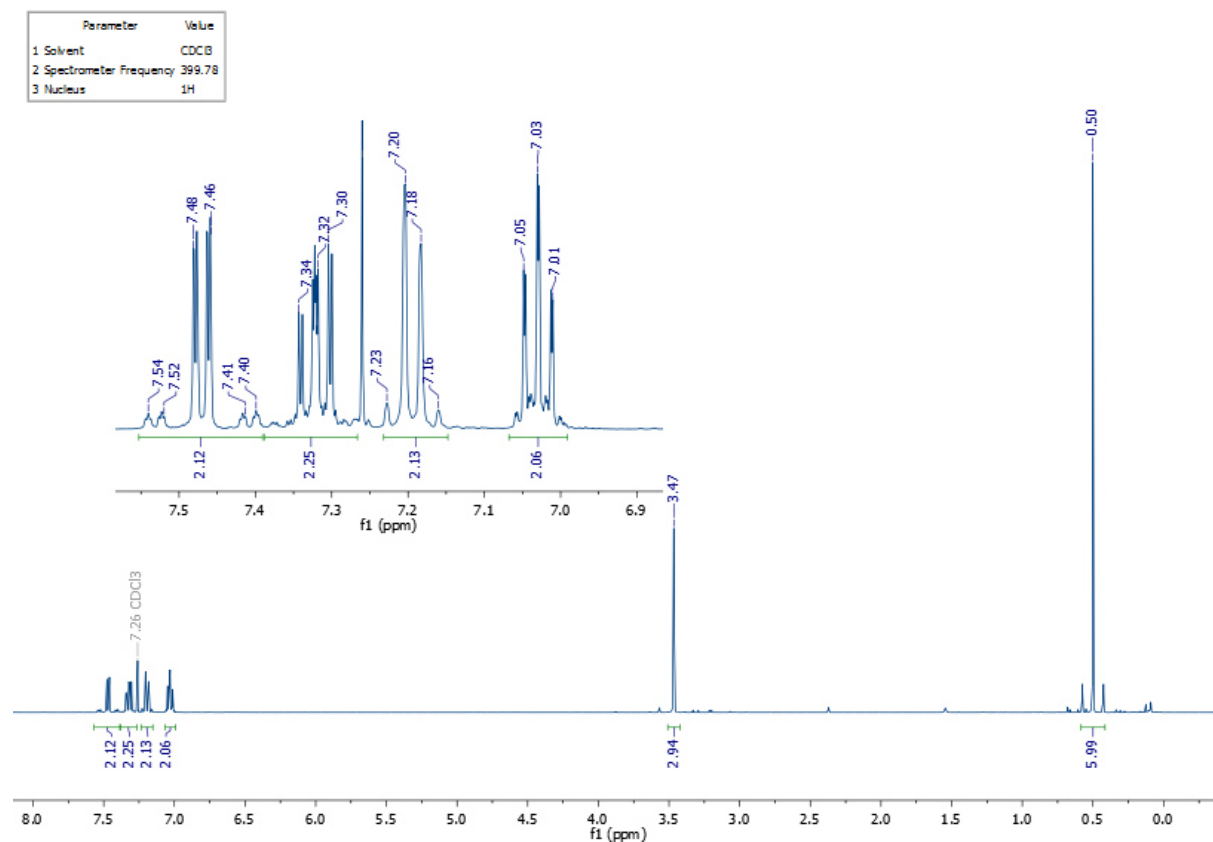


Figure S12 ¹H NMR spectrum of 5,10,10-trimethyl-5,10-dihydrophenazastannin.

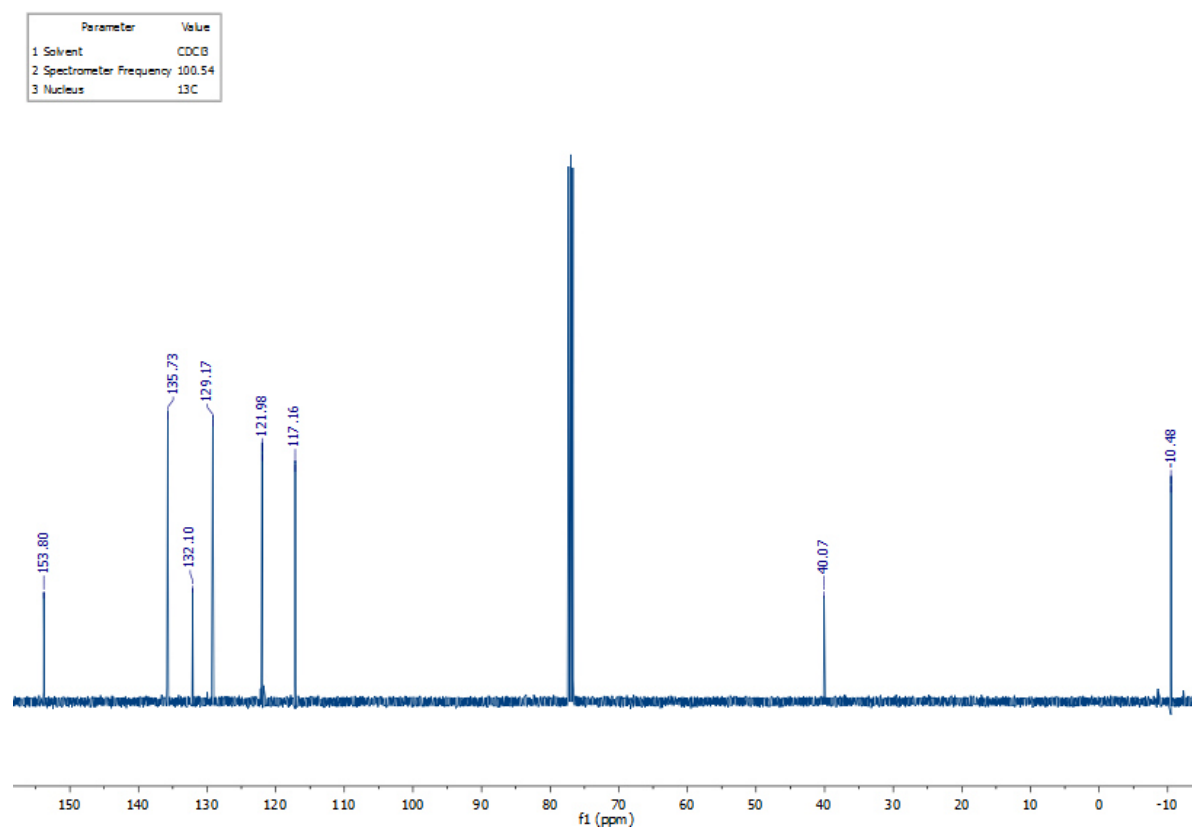


Figure S13 ¹³C{¹H} NMR spectrum of 5,10,10-trimethyl-5,10-dihydrophenazastannin.

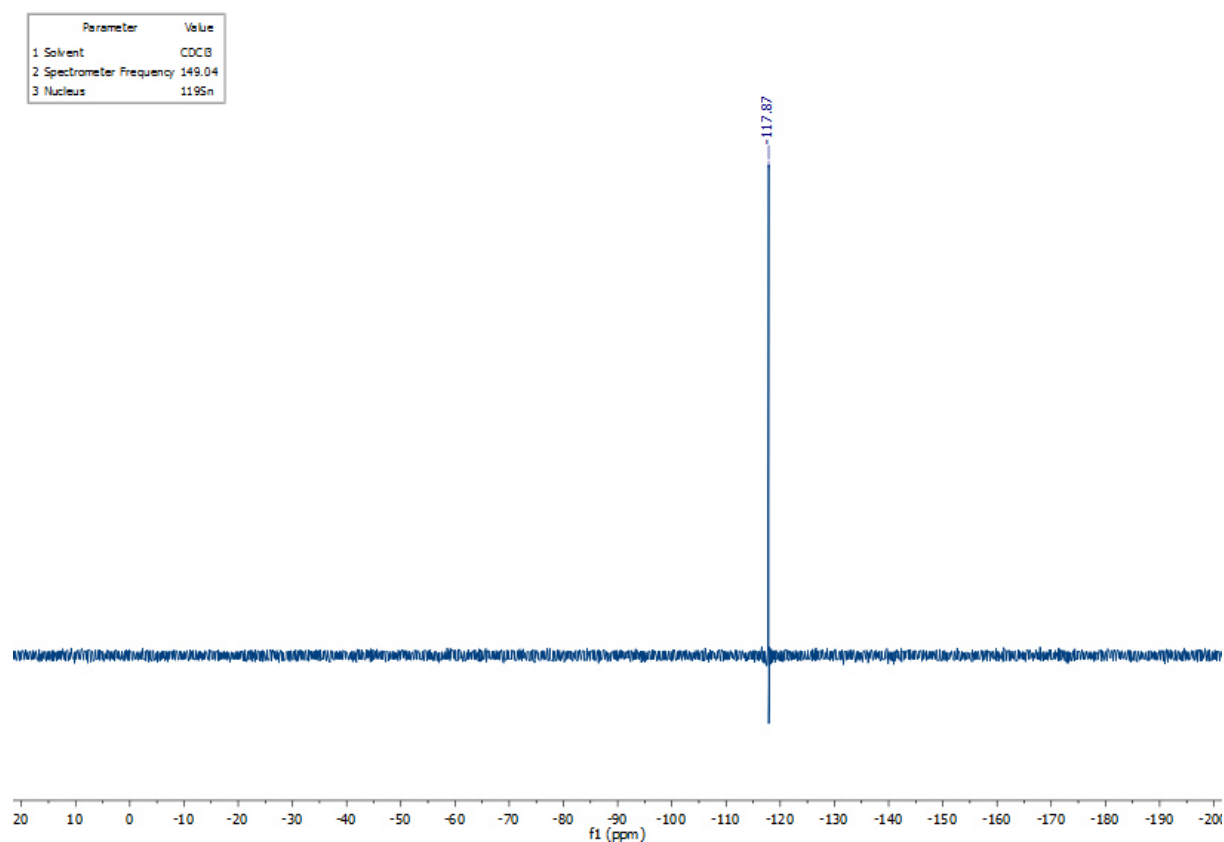


Figure S14 ¹¹⁹Sn NMR spectrum of 5,10,10-trimethyl-5,10-dihydrophenazastannin.

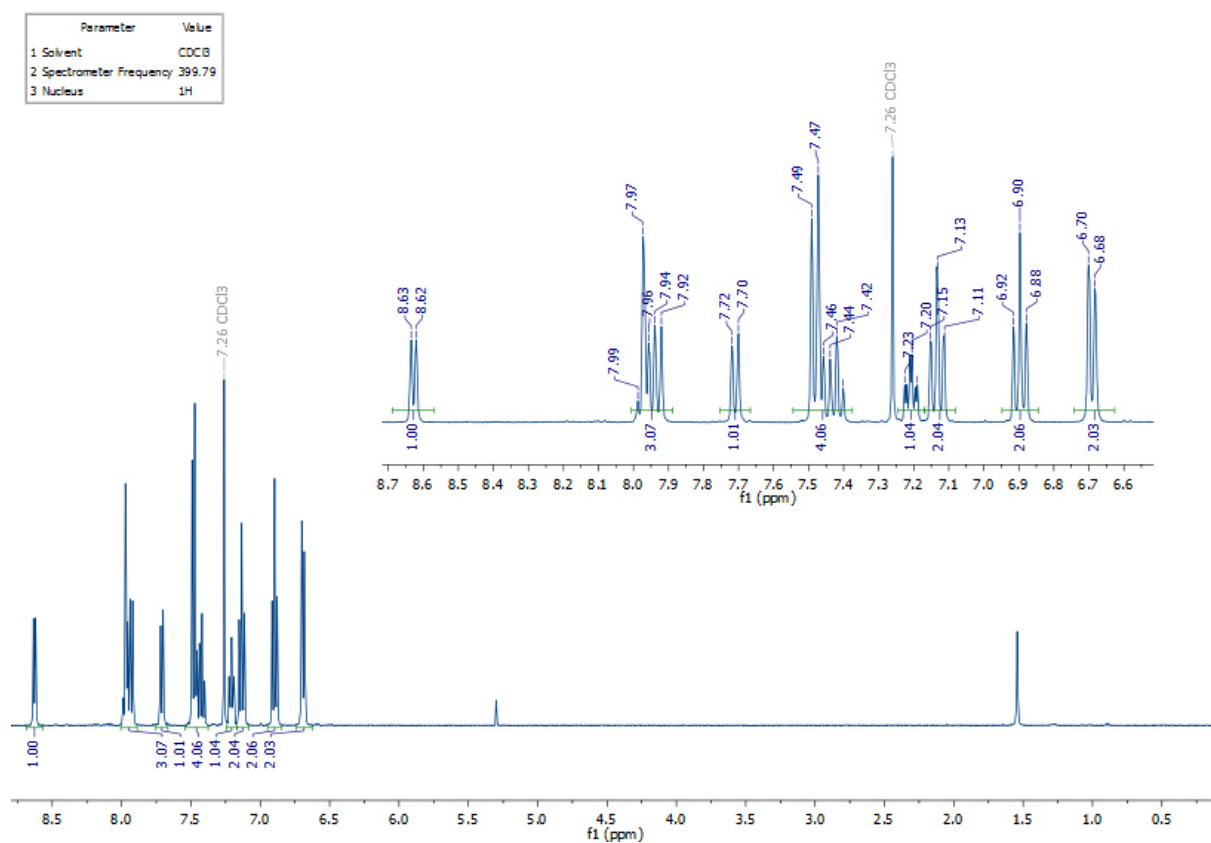


Figure S15 ¹H NMR spectrum of **1**.

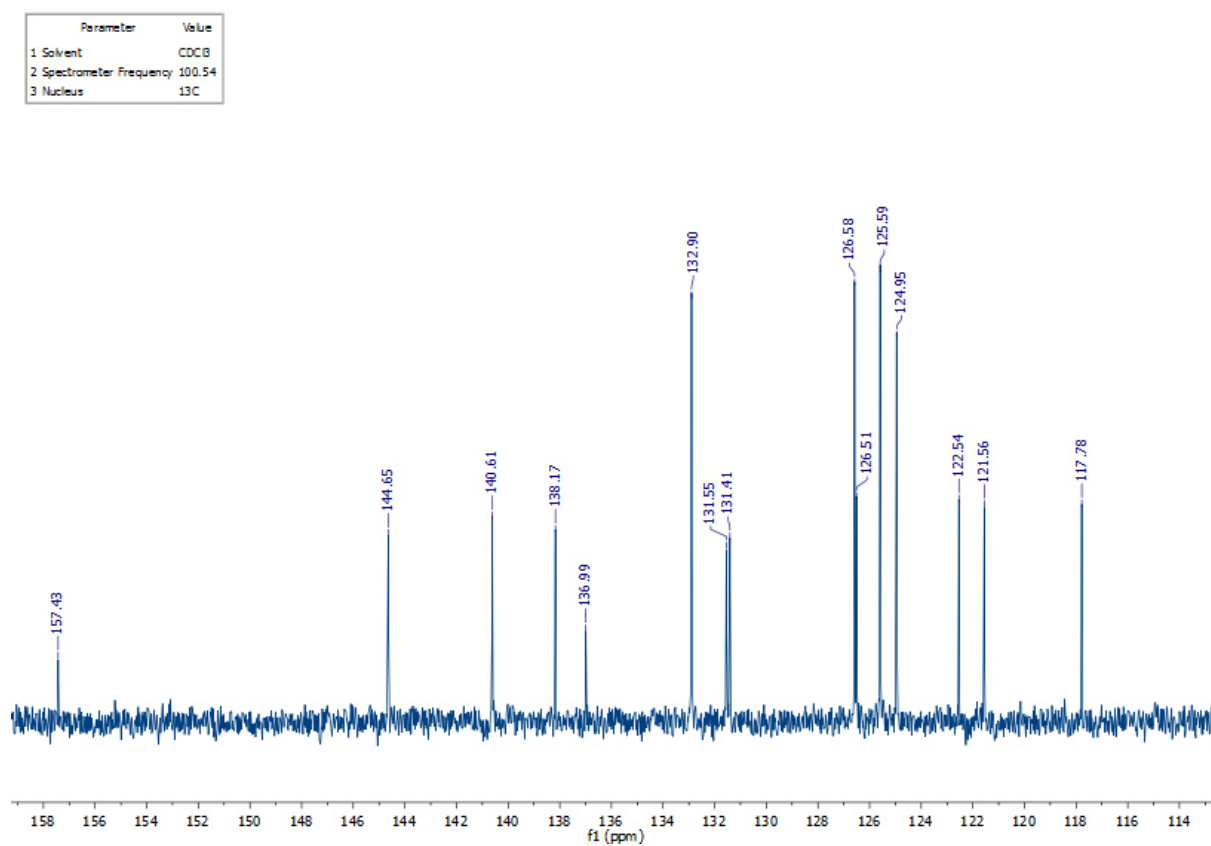


Figure S16 ¹³C{¹H} NMR spectrum of **1**.

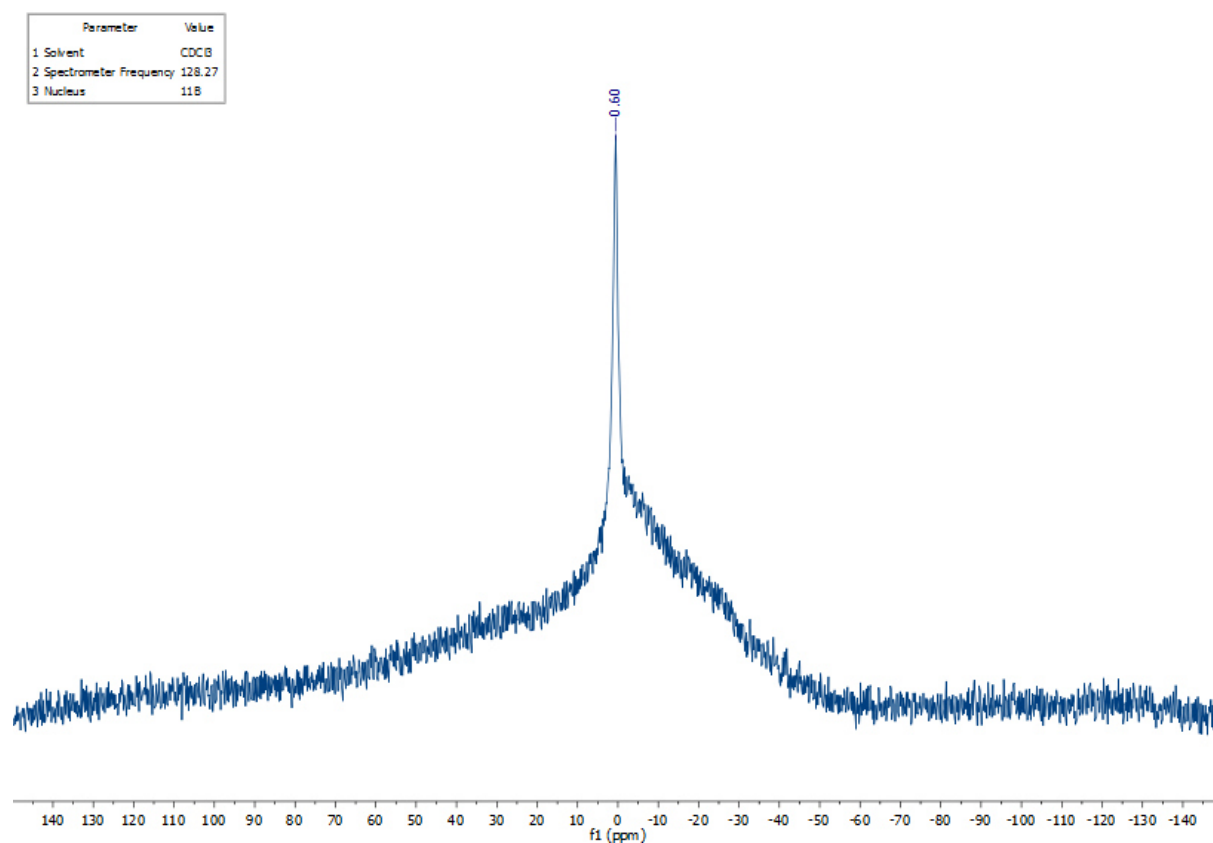


Figure S17 ¹¹B NMR spectrum of **1**.

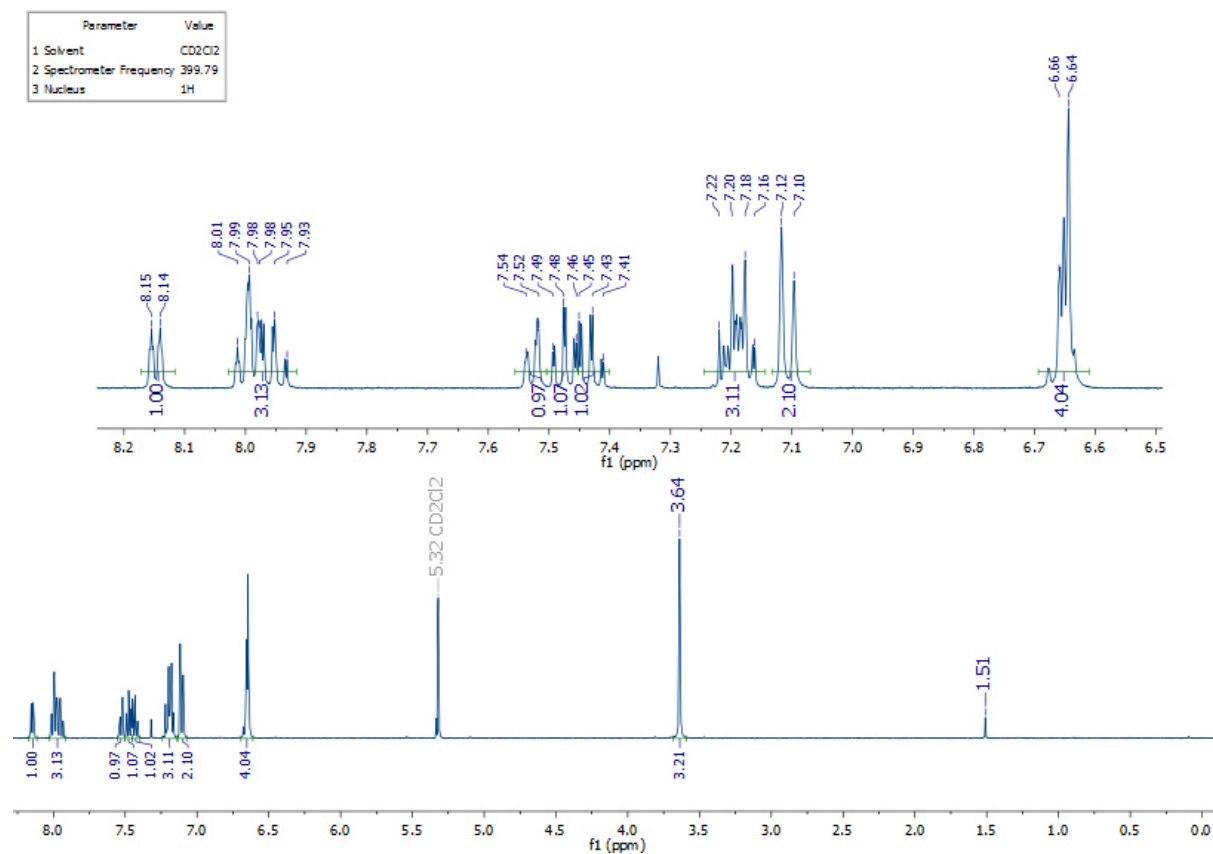


Figure S18 ¹H NMR spectrum of **2**.

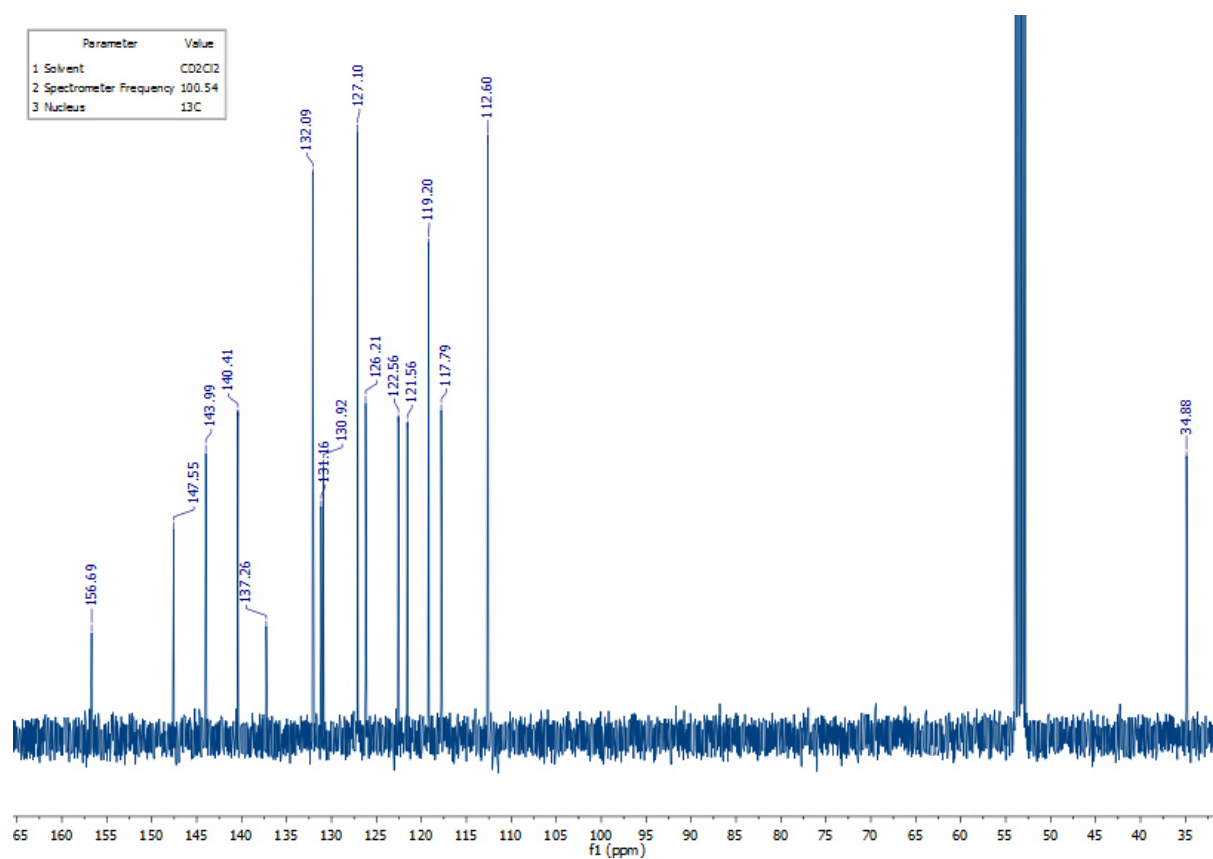


Figure S19 ¹³C{¹H} NMR spectrum of **2**.

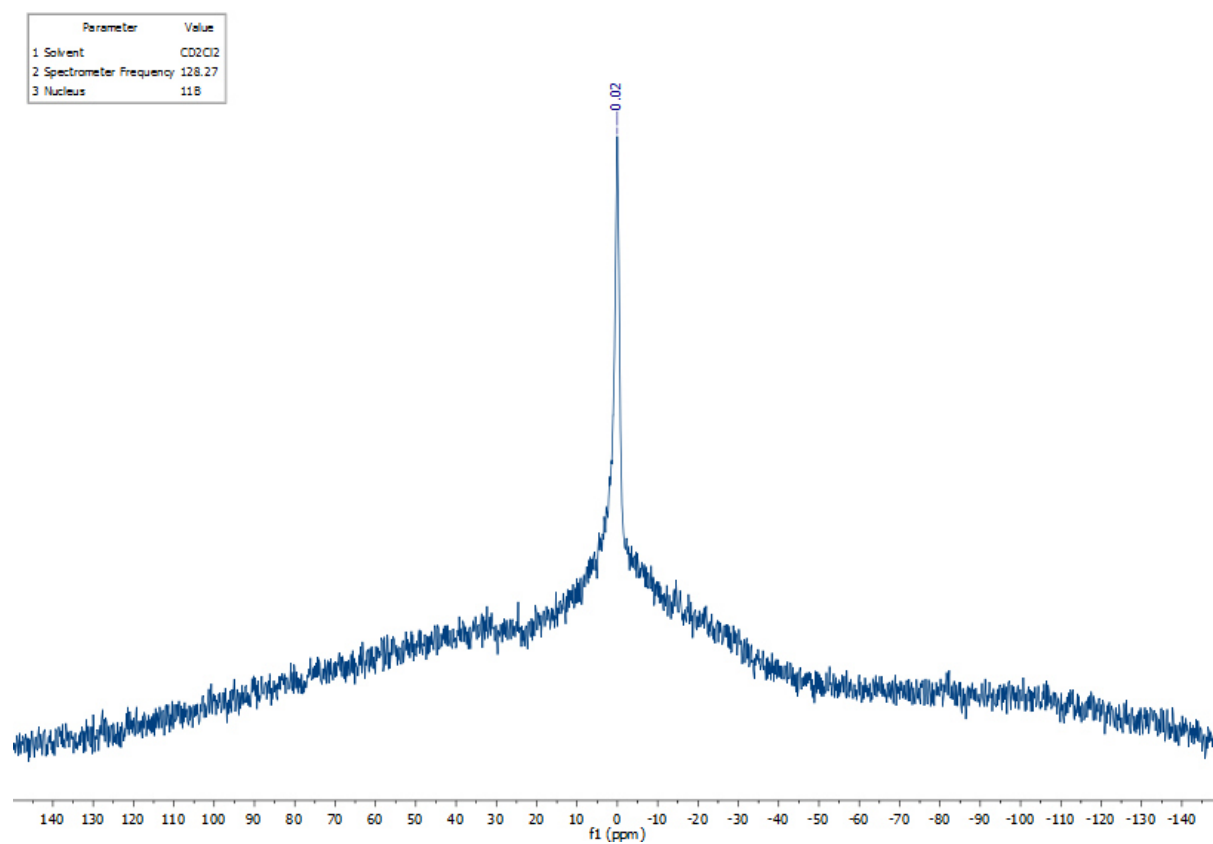


Figure S20 ¹¹B NMR spectrum of **2**.

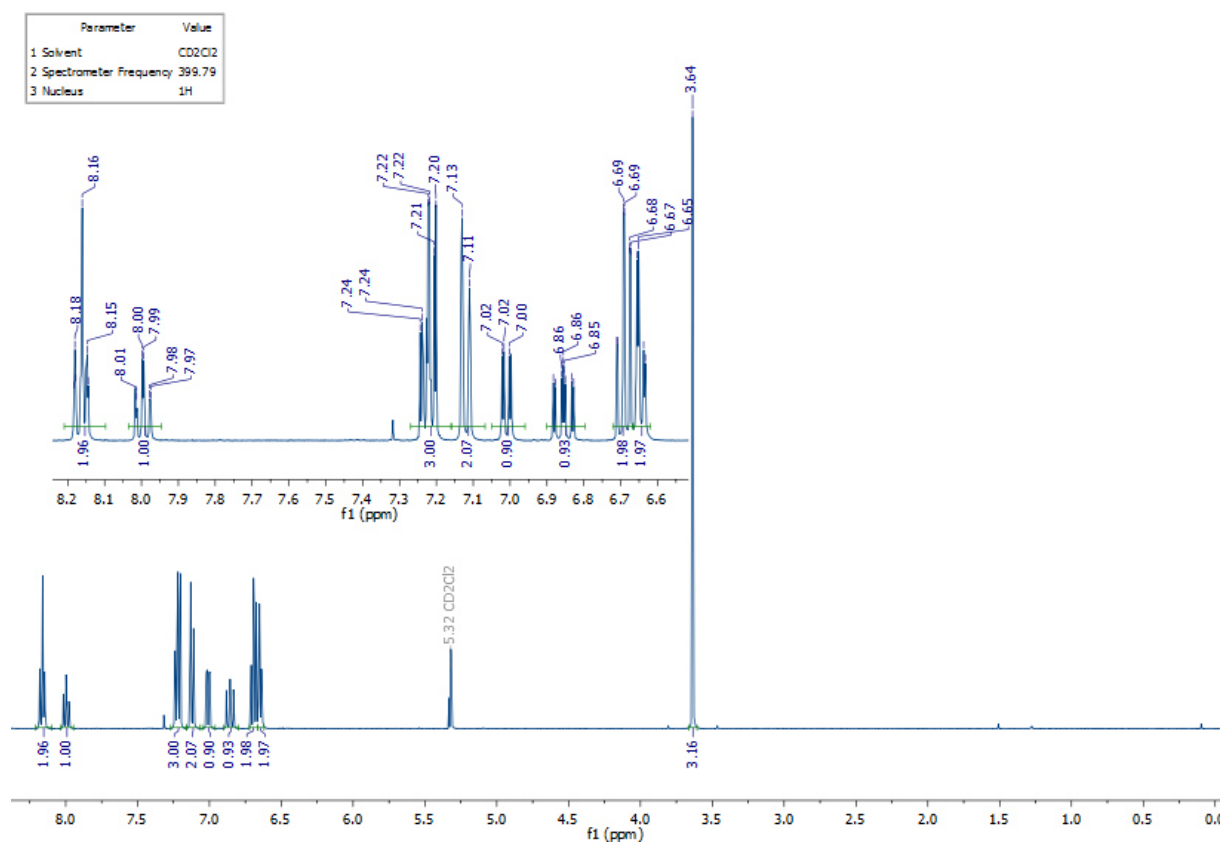


Figure S21 ¹H NMR spectrum of 2^F.

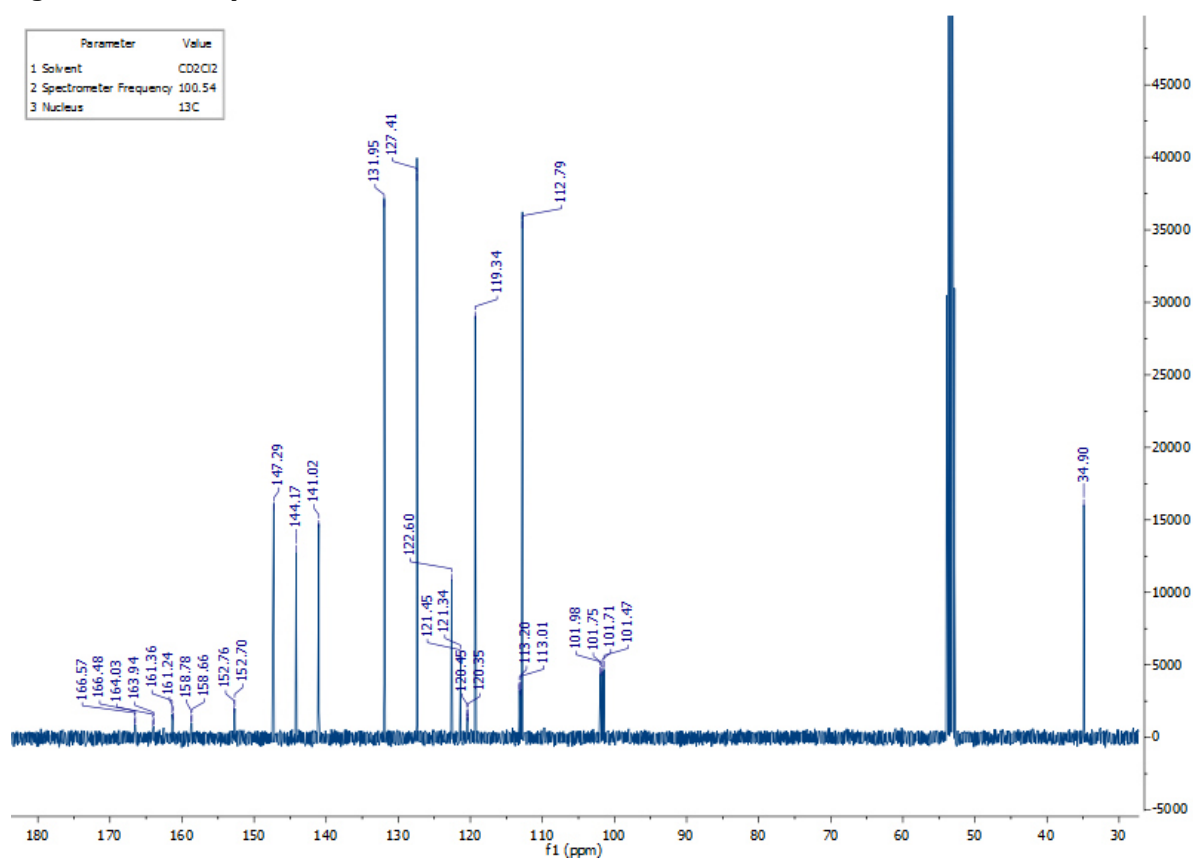


Figure S22 ¹³C{¹H} NMR spectrum of 2^F.

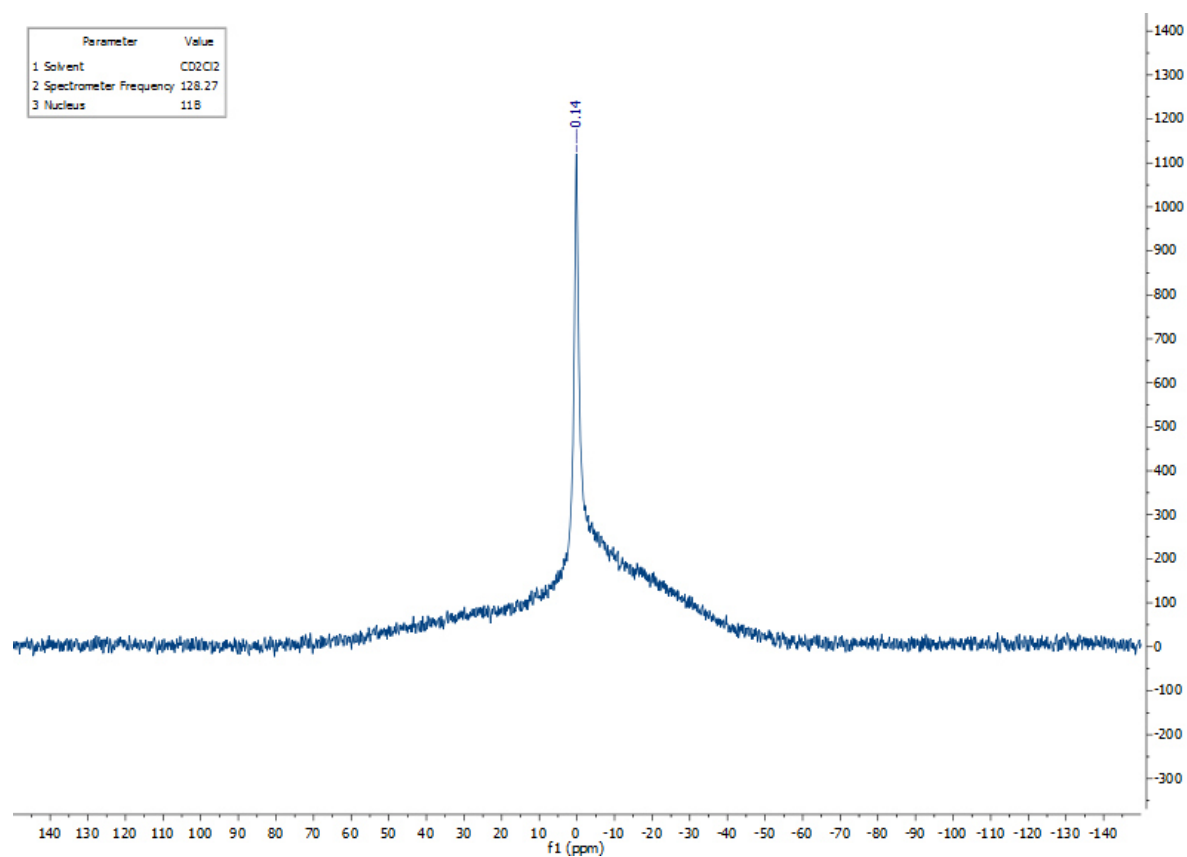


Figure S23 ¹¹B NMR spectrum of **2^F**.

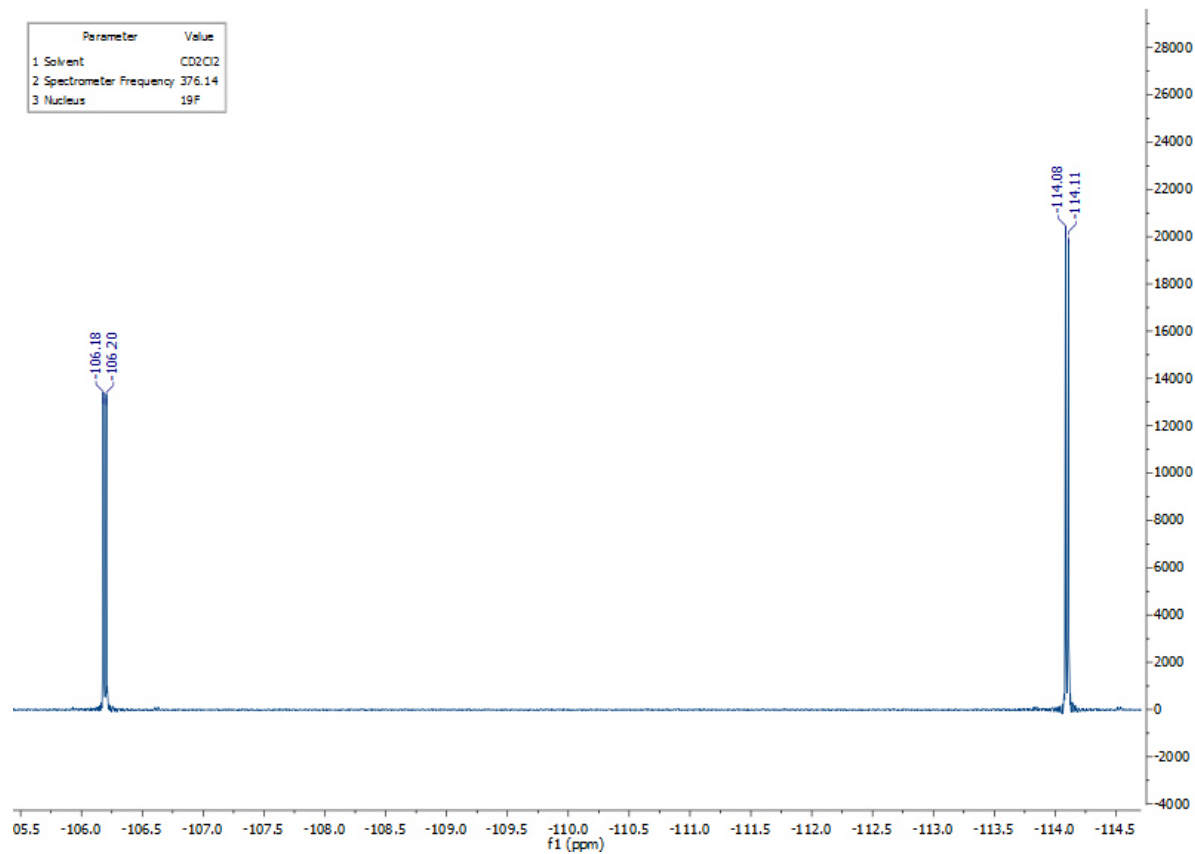


Figure S24 ¹⁹F NMR spectrum of **2^F**.

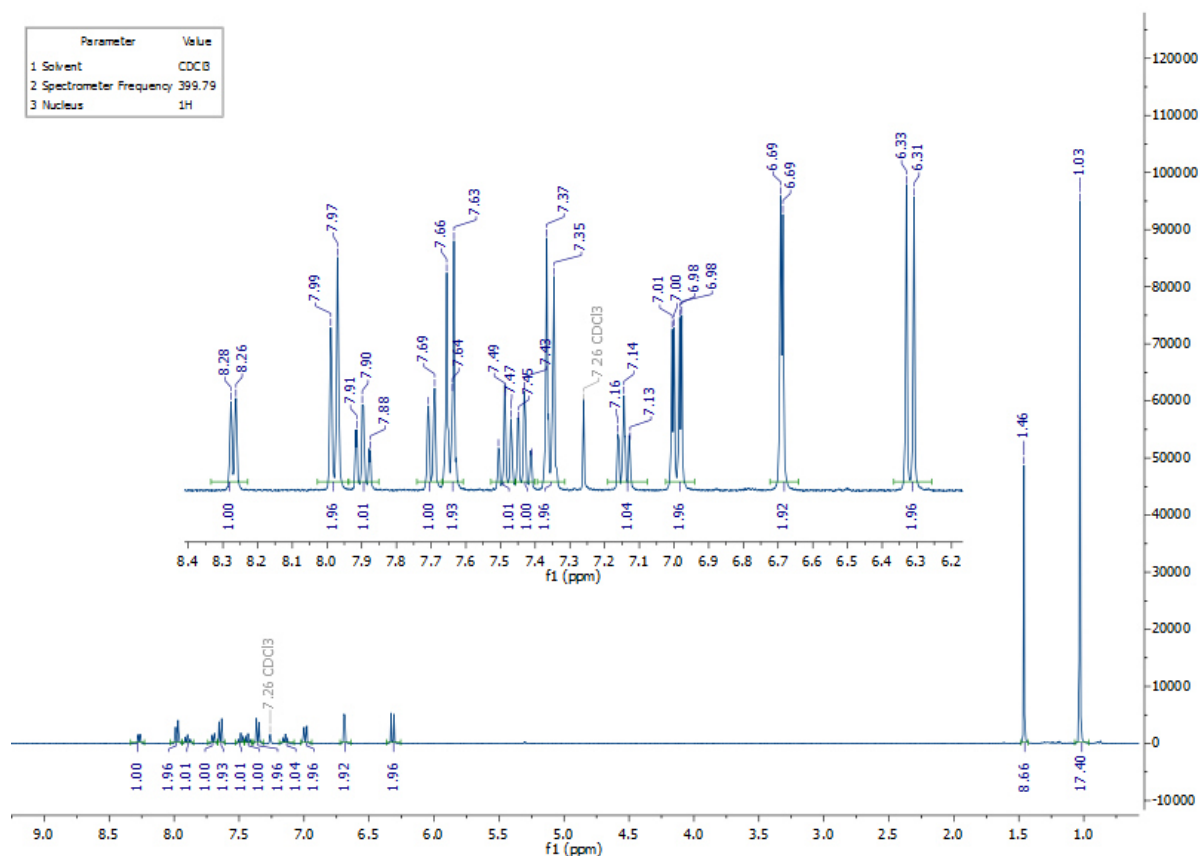


Figure S25 ¹H NMR spectrum of 3.

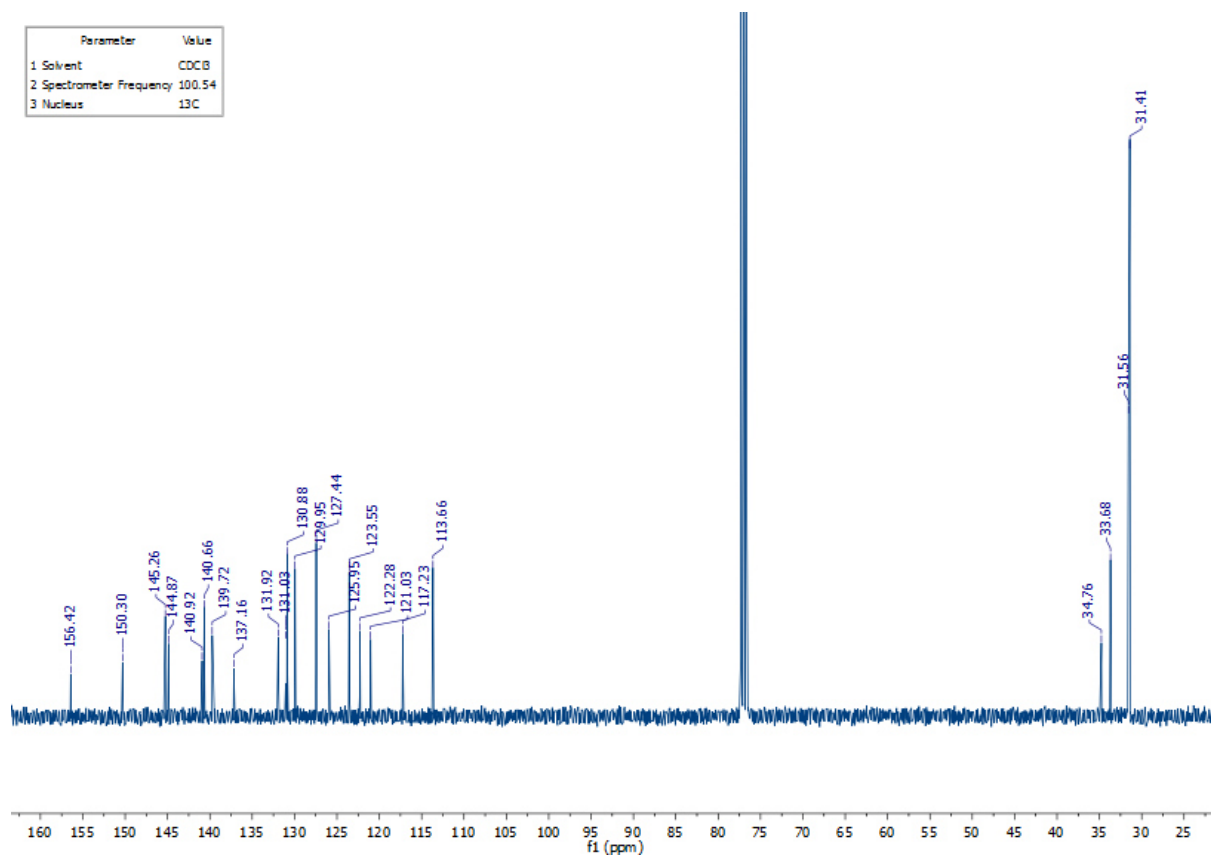


Figure S26 ¹³C{¹H} NMR spectrum of 3.

Parameter	Value
1 Solvent	CDCl ₃
2 Spectrometer Frequency	128.27
3 Nucleus	¹¹ B

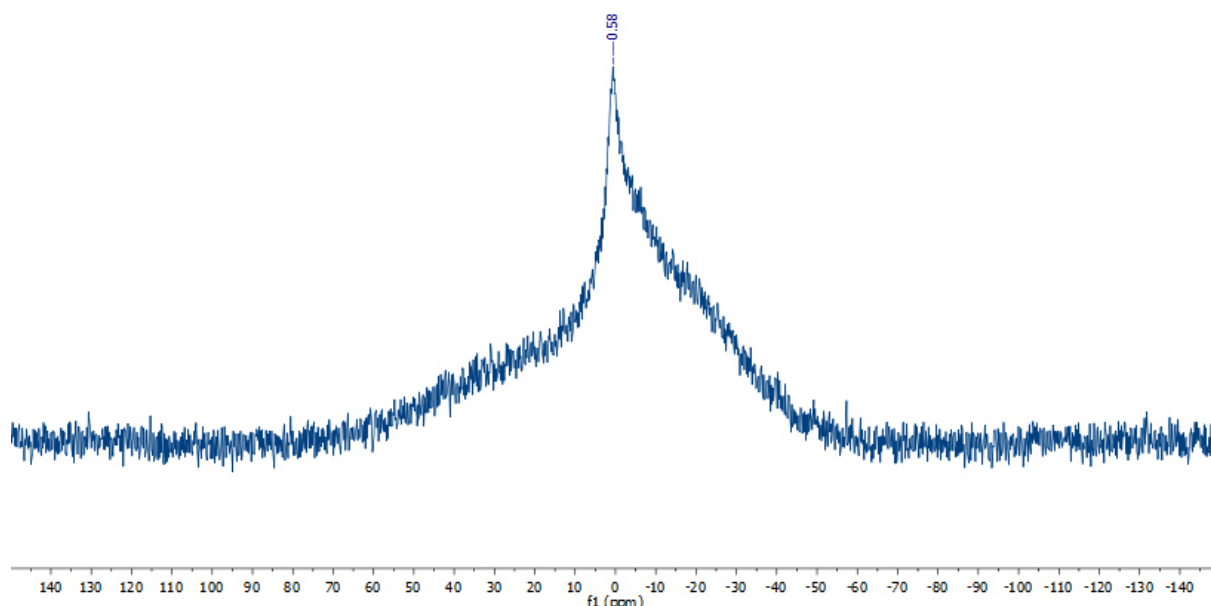


Figure S27 ¹¹B NMR spectrum of **3**.

S6 References

1. N. Ishida, T. Moriya, T. Goya and M. Murakami, *J. Org. Chem.*, 2010, **75**, 8709-8712.
2. Y.-J. Shiu, Y.-T. Chen, W.-K. Lee, C.-C. Wu, T.-C. Lin, S.-H. Liu, P.-T. Chou, C.-W. Lu, I.-C. Cheng, Y.-J. Lien and Y. Chi, *J. Mater. Chem. C*, 2017, **5**, 1452-1462.
3. A. Chopra, D. C. Dorton and C. A. Ogle, *Main Group Met. Chem.*, 1997, **20**, 783-786.
4. (a) R. K. Harris, E. D. Becker, S. M. Cabral De Menezes, R. Goodfellow and P. Granger, *Concepts Magn. Reson.*, 2002, **14**, 326-346; (b) R. K. Harris, E. D. Becker, S. M. Cabral De Menezes, P. Granger, R. E. Hoffman and K. W. Zilm, *Magn. Reson. Chem.*, 2008, **46**, 582-598.
5. H. A. Meinema and J. G. Noltes, *J. Organomet. Chem.*, 1973, **63**, 243-250.
6. M. R. Talipov, M. M. Hossain, A. Boddada, K. Thakur and R. Rathore, *Org. Biomol. Chem.*, 2016, **14**, 2961-2968.
7. B. M. Bell, T. P. Clark, T. S. De Vries, Y. Lai, D. S. Laitar, T. J. Gallagher, J.-H. Jeon, K. L. Kearns, T. McIntire, S. Mukhopadhyay, H.-Y. Na, T. D. Paine and A. A. Rachford, *Dyes Pigm.*, 2017, **141**, 83-92.
8. E. J. Kupchik and V. A. Perciaccante, *J. Organomet. Chem.*, 1967, **10**, 181-187.
9. G. M. Sheldrick, *Acta Crystallogr.*, 2008, **A64**, 112-122.
10. G. M. Sheldrick, *Acta Crystallogr.*, 2015, **C71**, 3-8.
11. O. V. Dolomanov, L. J. Bourhis, R. J. Gildea, J. A. K. Howard and H. Puschmann, *J. Appl. Crystallogr.*, 2009, **42**, 339-341.
12. A.-R. Allouche, *J. Comput. Chem.*, 2011, **32**, 174-182.
13. M. J. Frisch, G. W. Trucks, H. B. Schlegel, G. E. Scuseria, M. A. Robb, J. R. Cheeseman, G. Scalmani, V. Barone, G. A. Petersson, H. Nakatsuji, X. Li, M. Caricato, A. V. Marenich, J. Bloino, B. G. Janesko, R. Gomperts, B. Mennucci, H. P. Hratchian, J. V. Ortiz, A. F. Izmaylov, J. L. Sonnenberg, Williams, F. Ding, F. Lipparini, F. Egidi, J. Goings, B. Peng, A. Petrone, T. Henderson, D. Ranasinghe, V. G. Zakrzewski, J. Gao, N. Rega, G. Zheng, W. Liang, M. Hada, M. Ehara, K. Toyota, R. Fukuda, J. Hasegawa, M. Ishida, T. Nakajima, Y. Honda, O. Kitao, H. Nakai, T. Vreven, K. Throssell, J. A. Montgomery Jr., J. E. Peralta, F. Ogliaro, M. J. Bearpark, J. J. Heyd, E. N. Brothers, K. N. Kudin, V. N. Staroverov, T. A. Keith, R. Kobayashi, J. Normand, K. Raghavachari, A. P. Rendell, J. C. Burant, S. S. Iyengar, J. Tomasi, M. Cossi, J. M. Millam, M. Klene, C. Adamo, R. Cammi, J. W. Ochterski, R. L. Martin, K. Morokuma, O. Farkas, J. B. Foresman and D. J. Fox, *Gaussian 16 Rev. B.01*, Wallingford, CT, 2016.